BD Biosciences

Navigating the High-Content Imaging Process

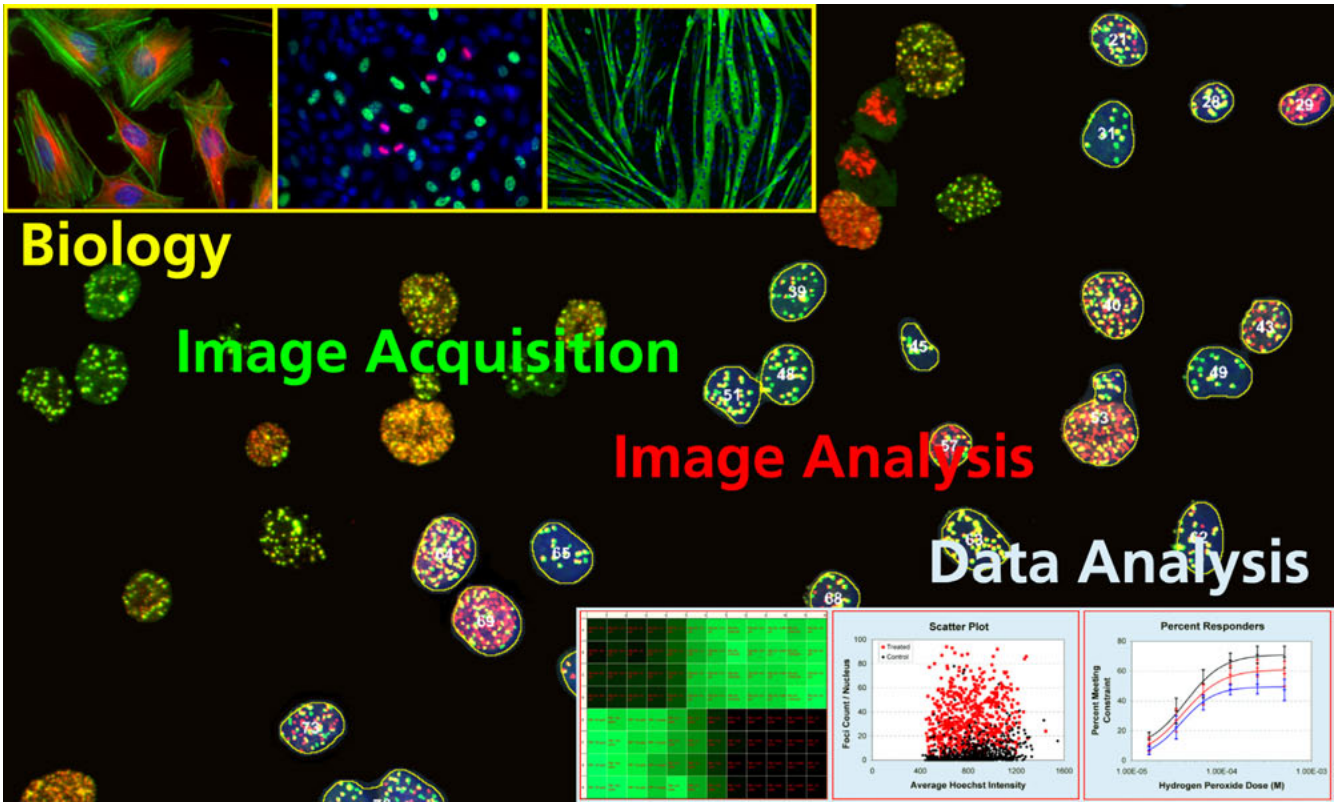

Introduction

High-content imaging is a rapidly growing field that has shown great potential in all phases of the drug discovery process.[1] Recently, high-content imaging has expanded to become a more widely used basic research tool. At the same time, applications of high-content imaging have broadened in scope, showing utility in systems biology, siRNA screening, and in other functional genomics and proteomics approaches. Whether one has extensive experience or is a novice in the field, navigating through the high-content imaging process is a complex task. A thorough understanding of the basic concepts, strategies, and goals of high-content imaging is crucial to ensure efficient and successful implementation of the technology. This application note examines some of the more important areas that should be considered when developing and optimizing a high-content imaging application.

High-content imaging can be characterized by the combining or multiplexing of two or more basic fluorescent microscopy experiments in which the biology has been adapted to multiwell plates and image acquisition and quantitative analysis have been fully automated. Simultaneous imaging of multiple cellular targets allows the extraction and analysis of numerous cellular features within a single experiment. The increased scale and speed of image acquisition and analysis required to perform high-content imaging demand a sophisticated instrumentation platform. BD Pathway™ high-content cell analyzers are designed and built specifically to run high-content imaging applications. The hardware and software of the BD Pathway systems allow maximum flexibility in image acquisition, analysis, and data visualization. Although specific capabilities vary between manufacturers of high-content platforms, many of the topics discussed in this application note apply generally to the high-content imaging field.

The high-content imaging process can be divided into four major stages: biology, image acquisition, image analysis, and data analysis. Within each stage are a number of factors that must be considered and optimized. Navigating through each stage involves the completion of a number of steps in which the successful completion of a step depends on the success of a previous step. When developing a new application, there are often many options to choose from to accomplish a specific task. The advantages and disadvantages of each option must be thoroughly examined and weighed. In addition, goals for the application should be well defined prior to initiating optimization and revisited frequently throughout each stage to ensure the factors and options selected accomplish the set goals.

BD Biosciences
15010 Broschart Road, Rockville, MD 20850
For more information visit **bdbiosciences.com/bioimaging**
Toll free: 800.245.2614 (US)
301.340.7320 (Outside the US)

Introduction *(continued)*

Table 1 lists the four major stages of high-content imaging and the key factors in each stage that may need to be optimized during the assay development process. Many of these factors are discussed in detail in this application note with specific examples from several high-content imaging applications However, within the scope of this application note, it was not possible to discuss every factor in detail, therefore, there may be additional factors that will affect your assay.

Table 1. Major stages of high-content imaging and key factors to be optimized.

Stage 1 – Biology

- Cells and Cell Culture
  - Media and Supplements
  - Primary Cells or Cell Lines
  - Suspension Cells
  - Whole Organisms
  - Live Cells (Kinetics Assay)
  - Fixed Cells (Endpoint Assay)
  - Passage Number
  - Plating Density
- Imaging Plates
- Extracellular Matrices
- Plate Setup and Compound Additions
- Plate Processing Protocols and Detection Reagents

Stage 2 – Image Acquisition

- Illumination Source
- Filter Sets
- Objective Lenses
- Camera Settings
- Image Resolution
- Number of Image Fields (Montage)
- Auto-Focus Methods
- Confocal Z Stack

Stage 3 – Image Analysis

- Image Processing
- Segmentation
- Measurement Features

Stage 4 – Data Analysis and Visualization

- Data Classification
- Heat Maps
- Scatter Plots
- Parameter Constraints
- Percent Responders
- Dose-Response Curves
- Z′-Factor
- Signal-to-Noise Ratio
- EC_{50}, IC_{50}

Stage 1 – Biology

One of the most important factors contributing to the success of a cell-based assay is the establishment and use of a robust and validated biological model. There are numerous factors to consider when choosing or developing a model system. Cells in culture are dynamic and should never be assumed to be a homogeneous population. Periodically the cells should be functionally tested to ensure they maintain desired characteristics and responses with increasing passage number. The cell culture medium and supplements are also critical to the performance of cells. Several different cell types and culture media should be considered and compared to select a combination that demonstrates the best overall assay performance. In addition, the extracellular environment plays a role in how cells adhere to the substrate, grow, and respond to drug treatments. The biological considerations are specific to each cell type, assay system, and analysis method, and therefore, must be optimized appropriately. Optimizing each of the many biological considerations at the onset of the assay development process will save a significant amount of time and effort overall.

Cells and Cell Culture

Choosing the proper cell type can have a major impact on assay results. The most relevant cells for the assay system should be chosen. Parameters, such as the species and tissue type of origin, as well as the presence or absence of specific signaling pathways, should be evaluated. Historically, options for cell-based assays have included cell lines and primary cells. Cell lines have been established from many different tissues and have been successfully used in a wide variety of cell-based assays. Cell lines, such as HeLa, U2-OS and CHO-K1, are readily available, fairly easy to propagate, and can proliferate in culture indefinitely. For such reasons, the vast majority of high-content assays have been developed using cell lines. Primary cells may theoretically provide a better model system because they are genetically and phenotypically more closely related to the *in-vivo* environment. However, these cells must be derived from animal or human sources, generally require more specialized growth environments, and can be maintained in culture for only a limited time. Therefore, primary cells generally are used only when the benefits outweigh the challenges. Stem cells, whether naive or differentiated, are potentially promising alternatives to both established cell lines and primary cells, but currently, the growth and maintenance requirements of these cells are not robust enough for most high-content applications.

Adherent cell lines grown as a cell monolayer are generally considered first for high-content imaging assays due to the relative ease with which they can be processed and imaged. However, alternative model systems, such as suspension cells, cells grown in multiple layers, or whole organisms, such as *C. elegans* or zebrafish embryos, can also be used to develop new high-content imaging applications. BD Pathway™ systems are uniquely suited to image these diverse and challenging sample types. For example, during image acquisition, the objective lens moves from well-to-well while the sample sits on a motionless stage. This facilitates the imaging of loosely attached cells and suspension cells by allowing them to remain undisturbed. In addition, flexibility in choice of imaging modes, such as wide-field, confocal, and montage, enables multidimensional imaging of a wide variety of biological samples (see the *Image Acquisition* section).

Another consideration is whether to use live cells (in kinetic assays) or fixed cells (in endpoint assays). With live cells, automated time-lapse fluorescent imaging and liquid handling operations can be used to observe cells in real-time as they respond to compound addition. The use of live cells in high-content applications generally requires additional time to develop, optimize, and implement assays. On the other hand, fixed-cell endpoint assays are easier to implement as they offer convenient stopping points and can be more highly automated to optimize sample throughput. Since many biological responses are transient in nature, it may be necessary to perform preliminary experiments with live-cells or with cells that have been fixed at different time points after treatment in order to investigate and optimize the kinetic aspects of a cellular response.

When measuring a biological response, control cells should have a low-basal level and high-response level while maintaining a high sensitivity to drug treatment. Increased passage number can change the properties of the cell line, such as response to stimuli, growth rates, protein expression, and signaling.[2] In the example shown in ***Figure 1***, high-passage HeLa cells showed less cytoplasmic to nuclear translocation of the NF-κB protein in response to tumor necrosis factor alpha (TNF-α) than low-passage cells. To ensure consistent assay results over time, cells should be maintained at relatively low-passage numbers. With increasing passage number, cells should be tested periodically for appropriate responses in the assay system.

Careful consideration should be made with respect to cell culture techniques. For example, placing newly seeded plates directly into a CO_2 incubator can cause an uneven distribution of cells in wells around the plate periphery.[3] In addition, incubating plates in suboptimal levels of humidity can cause unequal loss of medium around the edges of the plate due to evaporation. These anomalies, along with many others, can increase artifacts observed in edge wells (a phenomenon termed "edge effect") and contribute to plate-to-plate variation in assay results. Allowing newly seeded plates to sit at room temperature for approximately 30 minutes before placing them in a 37°C CO_2 incubator can produce a more even distribution of cells in each well, as described by Lundholt.[3] Maintaining an optimal humidity level in the incubator and using plates with evaporation lids and condensation rings, such as BD Falcon™ imaging plates (Cat. No. 353219), help prevent unequal loss of culture medium and can significantly reduce edge effect.

It is important to determine and plate the optimal number of cells for each application. Cell density within assay plate wells is dependent upon many factors, including cell size, growth rate, drug treatment, and how long the cells are to remain in culture. If cells are too sparse, additional image fields will need to be acquired to obtain a statistically significant number of cells. On the other hand, if cells are too dense, it may not be possible to segment them as single cells. ***Figure 2*** shows the effect of cell density on the ability to segment single cells.

Cell density also may affect how the population responds to drug treatment, and therefore has a significant effect on assay performance. Plating HeLa cells at 8,000 to 10,000 cells per well in a 96-well plate works well for applications in which the cells are imaged live or treated and fixed within 24 hours. This plating density also works for cells of a similar size and doubling time such as A549 and U2-OS cells. Cells of different sizes and with different doubling times require different plating densities. Applications in which cells are left in culture for extended periods will require optimization of the initial plating density. Finally, manual counting and plating of cells can lead to day-to-day variability in results, especially when performed by different people. An automated cell counting device, such as the BD AccuCell™ Automated Cell Counter (Cat. No. 350300), can remove variability from the cell counting process and provide more consistent day-to-day results. Variability can be further controlled with an automated cell plating device.

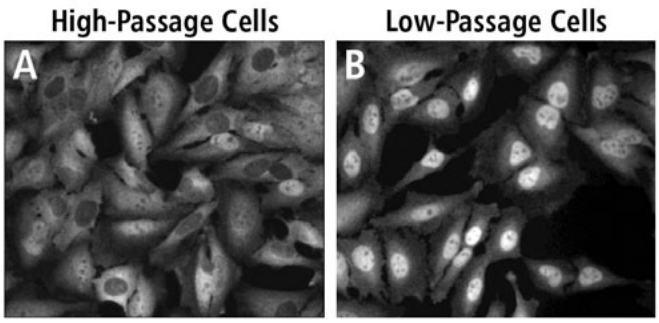

Figure 1. Loss of assay sensitivity in high-passage number cells. Cultures of high-passage (passage 32 after purchase, Panel A) and low-passage (passage 2 after purchase, Panel B) number HeLa cells were functionally tested in an NF-κB nuclear translocation assay. Cells were treated with TNF-α (50 ng/mL) for 30 minutes and subsequently processed for staining with an NF-κB antibody. In the higher passage cells, only a subpopulation of cells showed a positive response, as indicated by NF-κB antibody staining in the nucleus. In the culture of low-passage number cells, all cells showed a strong positive response. Images (cropped) were acquired using a 20x (0.75 NA) objective on a BD Pathway™ 855.

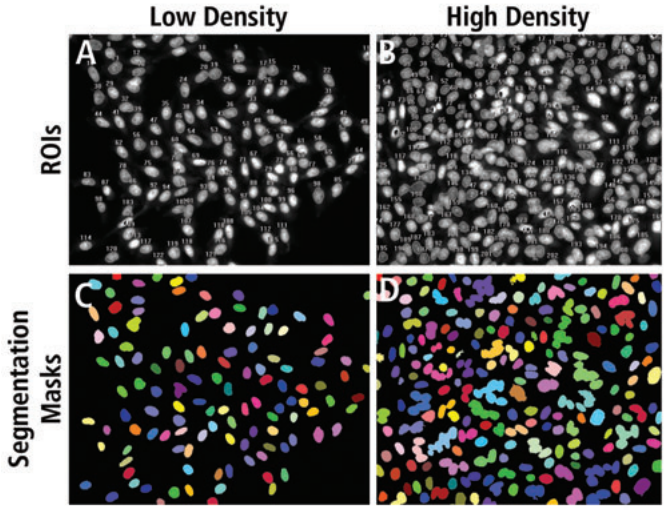

Figure 2. The effect of cell density on segmentation of single cells. CHO-K1 cells were seeded at low and high density. The next day, cells were stained with Hoechst and imaged. Images were segmented using BD AttoVision™ software which generated regions of interest (ROIs, Panels A and B) and segmentation masks (Panels C and D, colors randomly assigned). High-density cells (Panels B and D) were more difficult to segment to individual cells than low-density cells (Panels A and C). Images were captured using a 20x (0.75 NA) objective on a BD Pathway 435.

Imaging Plates

There are many types of multiwell plates. Choosing the appropriate plate is an important consideration; for instance, the type of imaging plate selected largely dictates the objective lens that can be used. ***Table 2*** lists the major advantages and disadvantages of different types of imaging plates.

Thick-bottom plates are generally >500 microns thick and require the use of long working distance (LWD) objectives to image through the sample. LWD objectives generally have a lower numerical-aperture (NA) value, which is a measure of light gathering ability and optical resolution (see the *Objective Lenses* section for more discussion of working distance and NA). Also, thick-bottom plates may produce more fluorescent background noise in images. However, thick-bottom plastic plates generally are flatter than thin plastic plates since the plate bottoms are more rigid. In addition, thick-bottom plates are available precoated (BD BioCoat™ plates) with a variety of extracellular matrices (ECM).

Thin-bottom plastic plates are typically <250 microns thick and can be imaged using high-NA objectives with short working distance capabilities. For example, the bottoms of BD Falcon™ 96-well imaging plates are ~190 microns. Because of the thinness of the plate bottom material and the relatively large distance across the wells (~6 mm in diameter), the imaging surface of thin plastic 96-well plates can be microscopically convex. The central region of the well of a thin-bottom plastic 96-well plate is the flattest part of the well (flatter than areas farther away from the center). Therefore, for best results, it is recommended to image at, or as close to, the center of the well as possible. With thin plastic 384-well plates, the area between wells is smaller, creating a flatter imaging surface.

As throughput needs increase, multiwell formats of greater than 96 wells can be used. Generally, transitioning from a 96-well plate to a 384-well plate provides sufficient increased throughput, however, 1536-well plates are also available. Transitioning from one plate format to another requires examination of all protocols including cell processing. For example, fixation and permeabilization protocols developed for a 96-well assay may not transfer directly to a 384-well format. While each well of a 384-well plate has roughly one-fourth the surface area and volume of a well of a 96-well plate, it is not always as straightforward as dividing all reagent volumes by four. In addition, 384-well plates are more difficult to work with in a manual mode. Therefore, instruments that provide automated dispensing and aspiration capabilities for cell plating and plate processing often are used with 384-well plates.

However, methods for these automated platforms must also be optimized. For example, automated plate processing equipment generally leaves behind some residual volume in each well. This potentially produce two negative effects: diluted reagent remaining in the wells which interferes with downstream steps and residual volume which dilutes the following reagent to a suboptimal concentration. The first effect can be resolved by using additional wash steps to further dilute the reagent to a point where it no longer has an effect. However, care should be taken to determine that the additional wash steps do not disturb fragile cell structures or loosely attached cells. Resolution of the second effect requires the use of more concentrated reagents to compensate for the dilution by the residual volume. ***Figure 3*** shows an example of an assay in which the 90% methanol permeabilization step that was effective in a hand-processed 96-well assay was ineffective when the assay was moved to an automation-processed 384-well format. Due to the ~10 µL residual volume created by the plate washer, the 90% methanol was diluted to a concentration below which it was an effective permeabilization reagent. When 100% methanol was used to bring the effective concentration to 90%, antibody staining was restored. These types of plate processing issues also can affect results when transitioning from standard volume plates to reagent conserving small volume or half area plates.

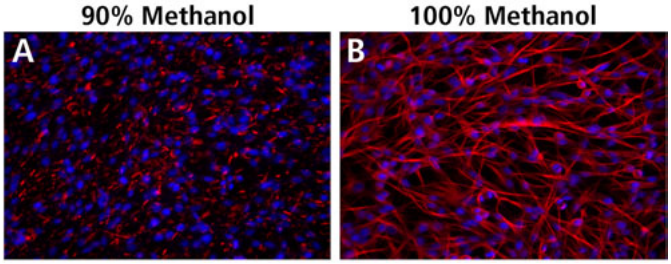

Figure 3. Comparison of methanol permeabilization buffer concentration on antibody staining in 384-well plates. 384-well thin-bottom plates (Cat. No. 353221) were processed using lab automation. C6 cells were fixed with paraformaldehyde, washed with PBS, and 100 µL of 90% methanol (Panel A) or 100% methanol (Panel B) was added prior to washing and staining with BD™ Bioimaging Certified Alexa Fluor® 555 mouse anti-β-tubulin antibody (Cat. No. 558605). Images of Hoechst (blue) and β-tubulin (red) labeled cells were acquired using a 20x objective (0.75 NA) on a BD Pathway™ 435 and color channel merged.

Table 2. Advantages and disadvantages of imaging plates.

Plate Type	Advantages	Disadvantages
Thick plastic >500 microns	• May be flatter than thin plastic plates • Available with a variety of coatings (BD BioCoat)	• Requires LWD (low-NA) objectives • Higher background fluorescence
Thin plastic <250 microns	• Relatively flat • Allows the use of high-resolution (high-NA) objectives	• May not be as flat as thick plastic
Glass <200 microns	• Flat • Allows the use of high-resolution (high-NA) objectives	• Higher cost • Cells may not adhere as well

Extracellular Matrices

Most commonly used adherent cell lines attach well to tissue-culture-treated plates. However, some cell types may not optimally adhere or spread on this type of surface. A variety of ECM, such as BD Matrigel™, collagen, poly D-lysine, or other surface coatings are available as precoated plates (BD BioCoat™) or as standalone reagents. Cells adhere differently to the various surface types. Loosely adhered cells or suspension cells, such as mouse lymphoma cells, may require a surface coating to maintain contact with the plate surface. A list of plate coatings recommended for a few specific high-content applications is provided in ***Table 3***.

Table 3. ECM for different applications.

ECM	Cells	Application
None	HeLa	NF-κB
Collagen	PC12 and SH–SY5Y	Neurite outgrowth
BD Matrigel	CHO–K1	Micronucleus
	HUVEC–2	Angiogenesis
Poly D-lysine	L5178Y (mouse lymphoma)	Micronucleus

The importance of using an appropriate ECM is demonstrated in ***Figure 4***. SH–SY5Y cells (a neuronal cell line) were grown in noncoated and collagen-coated plates and processed with paraformaldehyde and methanol. The number of cells retained on the plates was then quantified by counting Hoechst stained nuclei. After processing, >2.5–fold more cells were retained on the collagen-coated plate than on the noncoated plate.

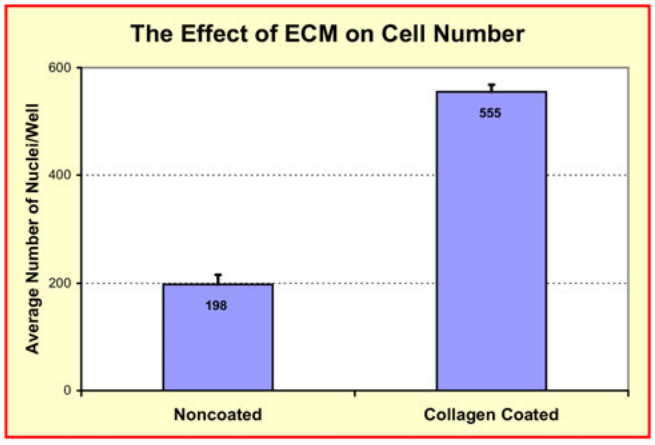

Figure 4. Comparison of noncoated and collagen-coated plates. An equal number of SH-SY5Y cells was plated and grown in noncoated and collagen-coated BD Falcon™ 96-well imaging plates. The cells were subsequently processed with paraformaldehyde and methanol. Images of Hoechst stained nuclei were segmented, counted, and the average number of nuclei per well plotted. N = 48 wells ± SEM.

Plate Setup and Compound Additions

To obtain robust and statistically significant assay data, careful planning of plate parameters, such as determining the number of replicate wells, should occur prior to running samples. Without adequate well replicates, confidence levels in the results are diminished and conclusions made from the data can be compromised. In addition, the position of replicates within the plate may also affect the outcome of an experiment. Data should be analyzed to determine if edge effect will bias the results. If the goals of the experiment are to determine assay window and robustness, then the assay plate should be prepared with a large number of both negative and positive control wells. Data generated from this type of plate setup can be used to calculate assay window (values from treated wells divided by values from control wells) and assay robustness (Z′-factor).[4] Alternatively, if the goal is to define assay sensitivity, the plate should be treated with a dilution series of relevant compounds at appropriate concentrations for a complete biological response. For optimal curve fitting, an adequate number of data points on each side of the midpoint need to be obtained. EC_{50} or IC_{50} values (see the *Data Analysis and Visualization* section) can be calculated from this type of plate set up.

Plate Processing Protocols and Detection Reagents

Whether employing live-cell or end-point assays, usually some sort of plate processing must be performed prior to imaging. Care should be taken to ensure that the plate processing steps do not compromise assay results. For example, mitotic and apoptotic cells are rounded up and more loosely attached to the plate surface. Therefore, if the culture medium is aspirated prior to fixation, mitotic and apoptotic cells can become detached and lost. Excessive cell loss during plate processing steps leads to under-representation of specific cell populations in the experiment. To minimize loss of loosely attached cells, a concentrated solution (2x or higher) of fixative can be added directly to the culture medium rather than removing the medium prior to fixation. Similarly, complex cellular structures, such as differentiated neurites, are very fragile and can easily break and lift off the plate surface during plate processing. ***Figure 5*** demonstrates the value of using reagents that reduce the number of wash steps on cells with fragile cellular structures. In this assay, the use of a directly conjugated antibody eliminated 40% of the wash steps and reduced disruption of the neurites. This was particularly evident at higher NGF concentrations when neural extensions became longer and more complex.

The choice of cell fixation and especially permeabilization reagents is crucial for optimal assay results. There are a variety of fixation reagents used for fluorescent microscopy. We have found that formaldehyde or paraformaldehyde (3.7% to 4%) works well for high-content applications. When performing antibody labeling of intracellular proteins, a permeabilization step must be used. The choice of permeabilization reagent, however, is a bit more complicated, as not all permeabilization reagents work optimally with all antibodies. ***Figure 6*** shows selected examples from a large antibody screen where Triton™ X-100 or methanol permeabilization was used for each antibody. For some antibodies, both permeabilization methods worked equally well; however, for others, only one method produced satisfactory results. Therefore, fixation and permeabilization methods and reagents should be optimized for the specific probes used in an assay. This is particularly important when multiplexing a variety of probes.

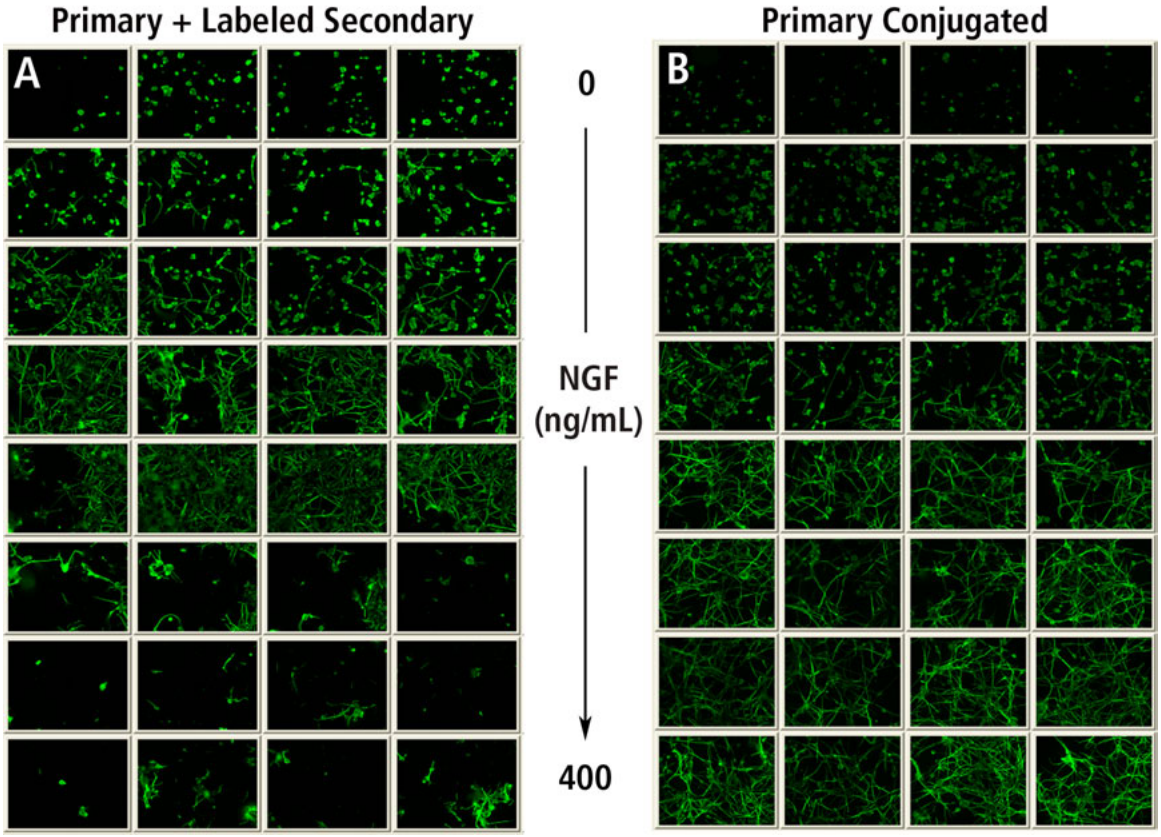

Figure 5. Comparison of reagents and protocols. PC12 cells were treated with increasing concentrations of nerve growth factor (NGF), as indicated, to differentiate neurite extensions. The cells were fixed, processed, and stained with a BD™ Bioimaging Certified β-tubulin antibody, which was either a primary β-tubulin (Cat. No. 556321) antibody followed by a labeled secondary antibody (Panel A) or a directly conjugated β-tubulin antibody (Cat. No. 558605, Panel B). Pseudocolored thumbnail images of four replicate wells for each NGF dose and antibody staining method are displayed. Images were acquired using a 20x (0.75 NA) objective on a BD Pathway™ 855.

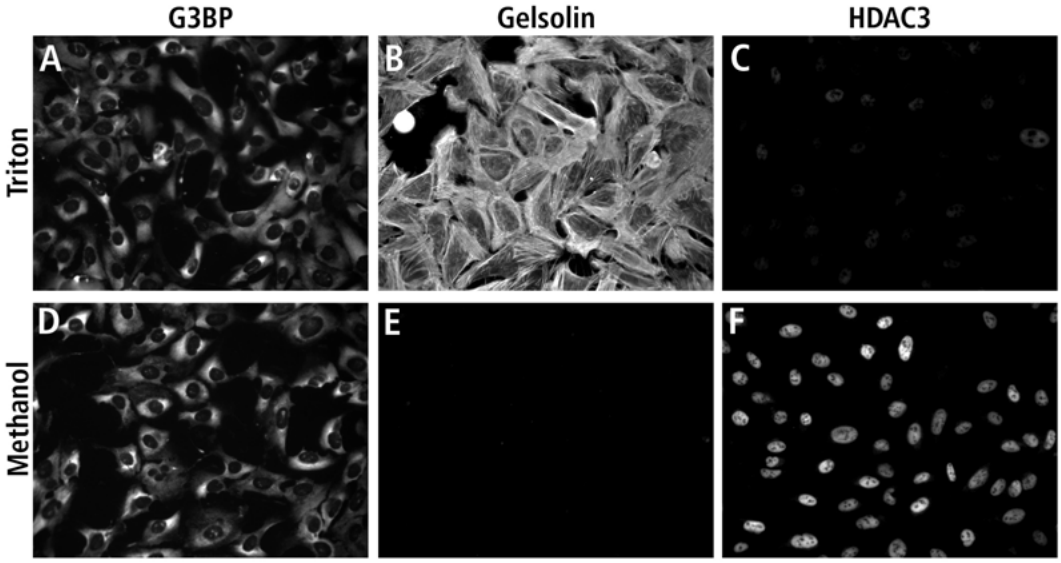

Figure 6. Comparison of antibody staining using different permeabilization methods. U2-OS cells were fixed with formaldehyde and subsequently treated with either 0.1% Triton X-100 (Panels A–C) or 90% methanol (Panels D–F). The cells were then stained with three different BD Bioimaging Certified mouse monoclonal antibodies. Antibody staining was detected using an APC-conjugated anti-mouse IgG secondary antibody (Cat. No. 550826). G3BP, a RasGAP SH3 domain binding protein (Cat. No. 611127, Panels A and D), showed the same staining pattern with both permeabilization reagents while Gelsolin, a protein with actin filament severing activity (Cat. No. 610413, Panels B and E), worked only with Triton X-100. HDAC3, histone deacetylase 3 (Cat. No. 611125, Panels C and F) worked best with methanol. Images were acquired using a 20x (0.75 NA) objective on a BD Pathway 855.

There is a rapidly growing list of reagents, fluorescent dyes, probes, and protocols available for use in biological research applications. However, a reagent that works in one application may not work in another. For example, a broad array of directly conjugated antibodies have been developed for use in flow cytometry, but in many instances these antibodies have been conjugated to dyes (such as FITC or PE) that are easily photobleached in a camera-based imaging system. Fluorescent dyes and probes used for high-content imaging should be chosen carefully for brightness, photostability, and compatibility with other reagents.

Immunofluorescent staining with antibodies is widely used to detect and localize molecular targets in individual cells, but many of the commercially available antibodies have not been tested for use in high-content imaging applications. In addition, the ability to multiplex antibody reagents is limited due to species cross-reactivity when using standard unlabeled primary antibodies with labeled secondary antibodies. To facilitate the use of antibodies for multiplexed high-content imaging applications, BD Biosciences initiated a screening process using automated imaging to evaluate monoclonal antibodies for their utility in bioimaging. This project initially included specificities that recognize proteins involved in cell signaling, cell cycle, apoptosis, and cancer. Antibodies relevant for neurobiology and embryonic stem cell applications have subsequently been screened. Antibodies were tested using cell lines and methods relevant to high-content screening applications on automated imaging platforms. Recommendations for the appropriate permeabilization method and concentration of antibody are included on the technical data sheet for each BD™ Bioimaging Certified Reagent. For more information about the development of BD Bioimaging Certified antibody reagents, refer to the application note "Screening and Development of Antibodies for Use in Cell-Based Assays Using Immunofluorescence Microscopy" available at: bdbiosciences.com/pdfs/whitePapers/07-A790030-18A.pdf.

Two distinct BD Bioimaging Certified Reagent product lines resulted from the antibody screening project. One is a large collection of unlabeled primary antibodies that have shown general utility in bioimaging applications. The other is a subset of these reagents that have been directly conjugated to multiple different fluorphores. The directly conjugated antibodies enable high-level (three or four colors) multiplexing in a variety of high-content imaging applications. For the most up-to-date listing of BD Bioimaging Certified Reagents go to bdbiosciences.com, and then perform a search for "bioimaging."

Fluorescent protein (FP) tags have proven to be invaluable research tools to investigate a wide variety of cellular processes, such as protein trafficking, gene activation, cellular differentiation, and development, and they are effective in high-content imaging. BD Biosciences has developed a set of Green FP and Red FP organelle vectors that can be used in both live- and fixed-cell imaging applications. These eight new BD Bioimaging Certified Reagents have been verified for proper expression and localization by examining their colocalization in cells using known antibodies and fluorescent dye reagents. For more information about FP reagents, refer to the application note "Fluorescent Protein Organelle Biomarkers are Beneficial in Live-Cell and Fixed-Cell–Based Imaging Applications" available at: bdbiosciences.com/appnote/FPorganelle.

Stage 2 – Image Acquisition

Once all biological aspects have been carefully considered and optimized, the next stage of a high-content imaging application is image acquisition. Just as in the biology stage, there are many different areas with multiple available options that must be investigated.

Illumination Source

The light source should be maintained and checked periodically for intensity and beam quality. Lamp intensity deteriorates with increasing hours of use; therefore, a lamp should be replaced as soon as its recommended life span is reached. The alignment of lamps requiring manual adjustments also should be checked periodically. Any change or adjustment to the light source or light path can impact assay results. For example, adjustments to the light path invalidate the current flat field correction reference images (see the *Flat Field Correction* section) and require new ones to be generated.

Filter Sets

There are a wide variety of filters for imaging the fluorescent probes and dyes used in high-content imaging applications. Filters are designed to transmit and reflect wavelengths of light in specific regions or bands of the color spectrum, which are also referred to as color channels. Filter sets should be matched carefully to the specific excitation and emission spectra of individual fluorescent dyes and probes. The standard filter sets in BD Pathway™ system filter wheels have been optimized for imaging a wide variety of commonly used fluorescent reagents that emit light in wavelengths ranging from UV to deep red color channels. Should the need arise, filters can be customized to accommodate more specialized applications.

Filters are classified based on their position within the optical path and are named according to the specific wavelengths of light they transmit. The wavelength range that a filter transmits is commonly referred to as the bandwidth or band-pass of the filter. Light that is not transmitted is reflected, and therefore is blocked or prevented from passing through the filter. Band-pass filters transmit light only between an upper and lower wavelength limit. For example, a 460/50 band-pass filter transmits light between 435 and 485 nm (a 50 nm band centered at 460 nm). Narrow band-pass filters transmit a relatively narrow band of light, for example a 360/10 filter transmits light between 355 and 365 nm. Long-pass filters transmit all wavelengths above a certain wavelength of light. For example, a 435LP filter transmits all wavelengths above 435 nm.

Standard epifluorescent microscopy utilizes three elements: an excitation filter, an emission filter, and a dichroic mirror. These same components are used in the filter wheels of the BD Pathway imaging systems (***Figure 7***). The excitation filter defines the wavelengths that illuminate the sample, while the emission filter allows only the appropriate wavelengths of light to be detected by the camera. The dichroic mirror, also called a dichroic beam splitter, is placed at a 45° angle and is located between the excitation and emission filters in the optical path. It directs excitation light to the objective and also acts to pass longer wavelength light from the sample to the emission filter. In the optical path of the BD Pathway 855, there is one additional filter wheel, the excitation dichroic wheel, which contains a full mirror, partial mirrors, a dichroic mirror, and an open position. The open position prevents light from Lamp A

from being blocked, which allows it to pass to the dichroic. The mirrors allow light to be either simultaneously or sequentially directed from the second mercury arc lamp (Lamp B) into the main optical path. With the dichroic mirror in place, two wavelengths of light can be switched using shuttering (rather than moving filter wheels) for applications requiring fast kinetic measurements such as calcium ratio imaging.

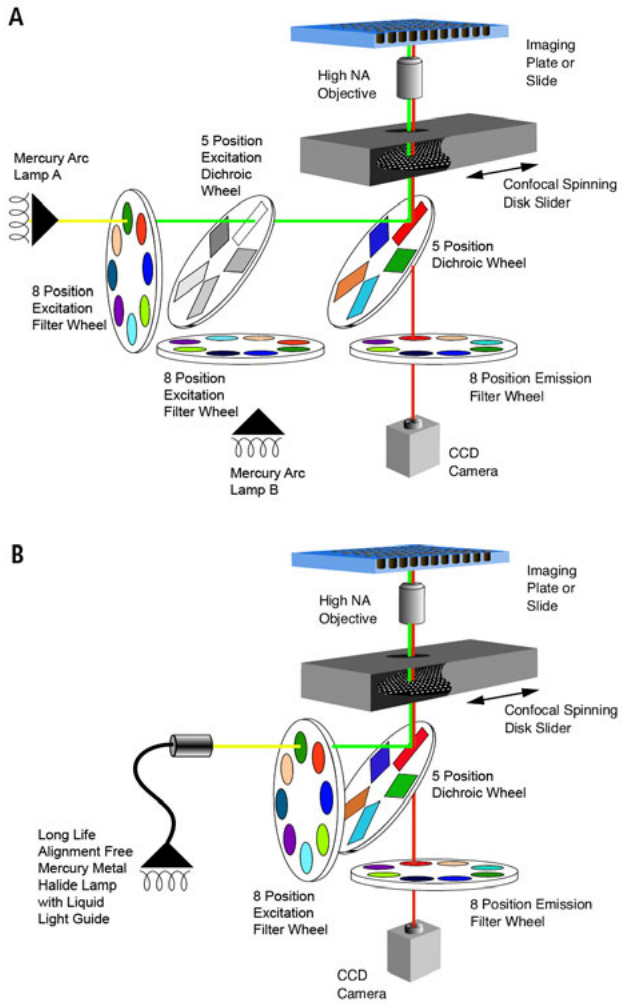

Figure 7. Optical path of the BD Pathway™ imaging systems. The BD Pathway 855 with illumination coming from Lamp A is shown in Panel A. Panel B shows the BD Pathway 435.

Most filter sets are designed for optimal imaging of a single color channel (single sets). Other filter sets are designed to transmit light in two or more color channels (multiband-pass sets), reflecting light between the colors they transmit. Long-pass and wide band-pass filters afford the highest light throughput, but may not be appropriate for use in multiplexed assays due to spectral bleed-through from the presence of fluorescent probes or dyes with overlapping excitation and emission spectra. Narrow band-pass filters and multiband-pass filters enable more efficient multiplexing; however, they transmit significantly less light due to the narrow transmission bands at each wavelength. Imaging with multiband-pass filters, therefore, may require relatively bright samples and longer exposure times than imaging with single color filter sets. The *Fluorescence Spectrum Viewer* shown in ***Figure 8***, is an online tool that can be used to optimize filter sets for multiplexed applications. This tool allows the excitation and emission spectra of many commonly available fluorescent dyes and probes to be viewed and plotted with different excitation and emission filters in order to determine the best combination. It also can be used to estimate the amount of spectral overlap or bleed-through that may occur with different combinations of probes and filters. The *Fluorescence Spectrum Viewer* can be accessed on the BD Biosciences web site at: bdbiosciences.com/spectra/.

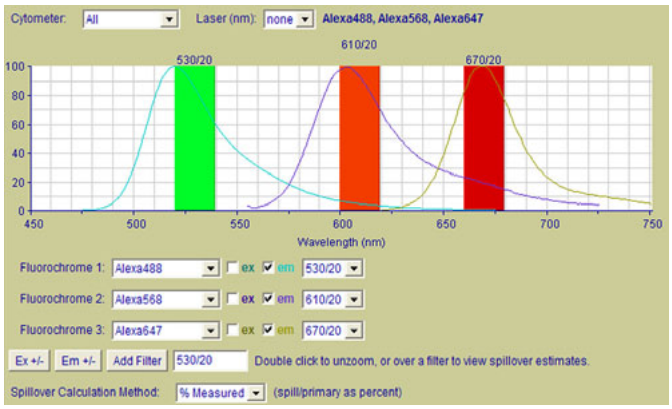

Figure 8. Screen shot of the Fluorescence Spectrum Viewer. The *Fluorescence Spectrum Viewer* is a useful tool for selecting appropriate probes and filter combinations for multiplexing high-content imaging applications.

Most high-content imaging data sets are composed of images of cells labeled with fluorescent reagents of multiple colors. The degree of colocalization between two or more proteins can be a useful measurement for some multiplexed applications. To visualize the spatial localization from two or more probes, it is helpful to overlay (merge) images of each color channel. However, in the merged image, one color may appear slightly misaligned relative to another. This phenomenon is termed pixel shift. Pixel shift may arise from misaligned filters and filter wheels or from the composition and properties of the individual filters. A slight shift in light passing through the different color channel filters can cause the image associated with one channel to shift on the camera chip relative to another channel. Pixel shift, when seen, is generally on the order of a few pixels. Therefore, only applications that require high-resolution images and precise colocalization of small objects, such as the colocalization of nuclear foci of DNA damage and repair, are impacted by pixel shift. Optical shifts also may be detected in the Z dimension where the optimal plane of focus is slightly different between color channels. Multiband-pass filter sets that utilize the same dichroic and emission filters for imaging different colors can be used to eliminate X, Y, and Z shifts between color channels. Or, if necessary, during the *Image Analysis* stage, images can be processed to correct for X and Y pixel shift. In addition, Z offsets can be defined within image acquisition protocols to accommodate different focal planes between color channels.

When developing and optimizing a new multiplexed, high-content imaging application, preliminary experiments should be designed to measure each of the filter characteristics discussed. To measure bleed-through, cells stained with each individual dye, as well as the multiplexed dyes, should be prepared and

imaged in the different color channels. In addition, experiments measuring specific signal intensity, nonspecific background, and pixel shift also should be performed. Based on the results of these experiments, appropriate adjustments to reagents, protocols, filter configurations, and other image acquisition parameters can be made.

Objective Lenses

Objective lenses are typically the most important component of an optical system because they are the predominant factor that defines image quality. Objective lens selection primarily depends on the resolution required for image analysis, the number of cells required to obtain statistically significant data, and, as previously mentioned, the imaging plate used (see the *Imaging Plates* section).

Objective lenses are primarily classified based on their magnification, working distance, and NA. The magnification of the objective needed for any given assay is determined by the image analysis needs of the assay. Measurements of structures over a large area, such as tubule formation in an angiogenesis assay or whole organism imaging, require imaging at low magnification (<10x magnification). Whereas, counting submicron nuclear foci in a DNA damage and repair assay requires high magnification (40x objective). Most high-content imaging applications fall somewhere in between requiring either a 10x or 20x objective. The ability to acquire four times more cells in the same number of image fields provides a distinct advantage when imaging with a 10x objective rather than a 20x objective; as long as the concomitant decrease in image resolution does not compromise image and data analysis. ***Table 4*** lists the field dimensions (measured using a micrometer on the BD Pathway™ 855) with representative assays suited for each objective lens. Image fields captured with objectives of different magnifications are shown in ***Figure 9***.

Table 4. Field dimensions and representative assays for objective lenses.

Objective	Field Dimensions (microns)	Representative Assay
40x*	210 x 160	DNA damage and repair
20x*	420 x 320	Nuclear translocation
10x	840 x 640	Cell cycle
4x	2100 x 1600	Tube formation
2x	4200 x 3200	Zebrafish imaging
* Both high-NA and LWD objectives are available for use on BD Pathway systems.		

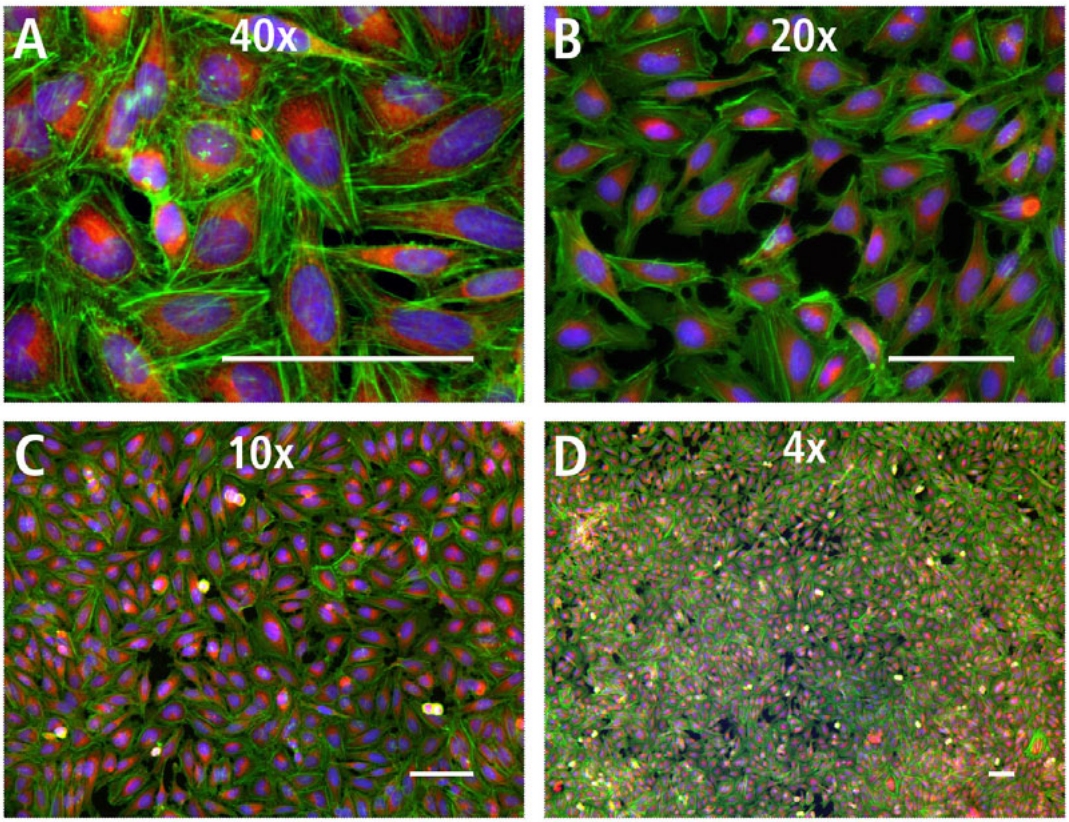

Figure 9. Comparison of images captured with objectives of different magnification. HeLa cells stained with Hoechst (blue), Alexa Fluor® 488 conjugated phalloidin (green), and MitoTracker® Red (red) were imaged with 40x (Panel A), 20x (Panel B), 10x (Panel C), and 4x (Panel D) objective lenses. If n equals the number of cells captured with a 40x objective, then the number of cells captured with a 20x, 10x, or 4x objective would be approximately 4 x n, 16 x n, and 100 x n, respectively. Full-field images (pseudocolored and merged) within the same well were acquired on a BD Pathway 435. Scale bars represent 100 microns.

The working distance of an objective is defined as the distance (in mm) from the front lens of the objective to the imaging surface (for example the distance between the objective and the sample) when the sample is in sharp focus. NA is a measure of the light-gathering ability of an objective lens. High-magnification lenses typically have high NA values and allow more image-forming light rays to enter the objective from wider (more oblique) angles. Therefore, high-NA objectives produce more highly resolved images than low-NA objectives. However, because of their short working distances, high-NA objectives can only be used with thin-bottom plates; they cannot be used to image samples in thick-bottom plates or plates with thick ECM coatings. Low-NA objectives (which have longer working distances) are required to image samples in thick-bottom plates. These objectives are, however, limited in terms of light-gathering ability and image resolution. The combined use of thick plates with low-NA objectives requires longer exposure times, and therefore may compromise the ability to image dim samples, especially in confocal mode.

Camera Settings

Camera settings, such as exposure time, pixel binning, and gain, are important factors that impact image quality and data analysis. Optimal camera settings must, therefore, be determined for each fluorescent dye or probe used in a high-content imaging application. Exposure times should be set so the brightest objects of interest are not overexposed (above the maximum pixel intensity). Saturated pixels in an image can compromise the accuracy of subsequent intensity-based measurements. When imaging dim samples or imaging in confocal mode, in which significantly less light is transmitted to the camera, pixel binning and camera gain settings can be used to shorten exposure times. However, if applied inappropriately, both of these camera adjustments can adversely affect image quality.

The term bit depth, also called pixel depth, refers to the maximum number of intensities that can be displayed by the camera at one time. The charge-coupled device (CCD) camera in BD Pathway™ systems produces 12-bit images (2^{12} or 4096 shades of gray) consisting of an array of 1344 x 1024 pixels (for the BD Pathway 855) or 1392 x 1024 pixels (for the BD Pathway 435). There is a set number of photoelectrons that must register to a pixel for each gray level. Objects that emit fewer photoelectrons (dim samples) register fewer gray levels than objects that emit higher numbers of photoelectrons (bright samples). The camera exposure should be set to maximize the dynamic range of the gray level values. For example, working with a 12-bit camera on a BD Pathway, the exposure should be set so the maximum pixel intensities of the brightest signal is between 3500 and 4000 gray levels (scale 0 to 4095). For dim samples, camera exposure should be set to obtain sufficient signal to achieve an adequate separation between the specific and nonspecific (background) intensities. Although the images acquired by the cameras contain 12-bits of data (4096 shades of gray), they are stored unaltered (without scaling) in 16-bit data files in order to be compatible with commonly used image processing software.

The camera gain adjustment defines the number of accumulated photoelectrons that determine each gray level. An increase in electronic gain corresponds to a decrease in the number of photoelectrons that are assigned per gray level. This differs from gain adjustments applied to other types of detectors (such as photomultiplier tubes used in flow cytometers) that amplify signals using a fixed multiplication factor. Camera gain allows a given signal level to be divided into a larger number of gray level steps. Although gain adjustment provides a method to expand a weak signal to a desired larger number of gray levels, excessive use of camera gain can lead to increased levels of noise which appear as graininess in the final image.

Combining pixels in the camera array is referred to as pixel binning. In an unbinned image (referred to as bin 1 or 1 x 1 binning), each of the camera pixels is measured independently. At bin 2 (2 x 2 binning), four adjacent pixels are combined into one larger pixel or superpixel. At bin 4 (4 x 4 binning), 16 pixels are combined, and so on. The resulting superpixels are processed as a single pixel that contains the combined photoelectron content of all the combined pixels. The benefits of pixel binning are increased signal intensity that enables exposure times to be reduced by ~4–fold (per bin level) and smaller image file sizes that reduce both data storage demands and image processing time. However, with each increased bin level, spatial resolution decreases. Generally, images obtained using bin levels greater than 2 x 2 are not useful for quantitative image analysis. High-bin levels (4 x 4 or 8 x 8) are useful, however, to increase the speed of image-based auto-focus methods.

Image Resolution

Image resolution is a term used to describe the level of detail contained in an image and is primarily determined by the magnification of the objective and the number and dimensions of the pixels in the camera and image. Field dimensions of individual objective lenses used on an imaging system can be measured with a micrometer. Image resolution (in microns/pixel) then can be calculated by dividing the field dimensions (in microns) by the image dimensions (in pixels). Field dimensions measured for different objectives on the BD Pathway 855 were used to calculate image resolution at different levels of pixel binning and are listed in ***Table 5***. Imaging at bin 1 with a 20x objective generates images with a similar image resolution (0.3125 microns/pixel) as imaging at bin 2 with a 40x objective. Since the field of a 20x objective is four times larger than the field of a 40x objective, four times more cells can be captured per image field. This can be advantageous for applications that demand both high resolution and higher numbers of cells since acquisition times can be significantly decreased. Imaging at bin 1, however, requires a longer exposure time than imaging at bin 2, which may increase background noise in images and compromise assay results.

Table 5. Image field dimensions and characteristics captured with different objectives and levels of pixel binning.

Binning	Image Dimension (pixels)	Image File Size (KB)	Objective	Field of View (microns)	Resolution (microns/pixels)
1 x 1	1344 x 1024	2697	40x	210 x 160	0.15625
			20x	420 x 320	0.3125
			10x	840 x 640	0.625
2 x 2	672 x 512	677	40x	210 x 160	0.3125
			20x	420 x 320	0.625
			10x	840 x 640	1.25
4 x 4	336 x 256	171	40x	210 x 160	0.625
			20x	420 x 320	1.25
			10x	840 x 640	2.5
8 x 8	168 x 128	44	40x	210 x 160	1.25
			20x	420 x 320	2.5
			10x	840 x 640	5.0

Number of Image Fields (Montage)

In high-content imaging, it is important to capture a large enough population of cells in each image to obtain statistically significant data. The number of cells acquired is determined by the type and number of cells plated and the magnification and number of image fields captured. Acquisition of larger numbers of cells in each well or image generally translates into an assay with higher statistical significance as measured by Z′-factor (see the *Data Analysis and Visualization* section). Assays with a Z′-factor value of >0.5 are considered significantly robust for screening applications.[4] Since many cell-based biological responses are heterogeneous, increasing the size of the analyzed cell population decreases the variation of well mean data measured in replicate wells and increases Z′- factor values. One way to increase the number of cells analyzed is to increase the cell plating density. However, high-content imaging applications generally analyze single cells rather than the cell population and high-density plating can hinder single-cell segmentation. An alternative is to image additional fields through the use of either contiguous or discontiguous montage. In contiguous mode, BD Pathway™ systems can precisely acquire adjacent image fields and combine them into a single larger multifield montaged image for analysis. This is particularly useful in the neurite outgrowth assay as shown in ***Figure 10***. This assay has inherently low-Z′-factor values due to the heterogeneous nature of the extended neurons. This is compounded by the long cell processes that extend beyond the borders of a single image field. The data shows that with increasing contiguous montage size, the Z′-factor values increased for each of the assay parameters measured by the BD AttoVision™ Neurite Outgrowth application software. A 4x4 montage enabled Z′-factor values of >0.5 to be obtained. For more detail, refer to the "Quantitative High Content Analysis of Neurite Outgrowth" application note available at: bdbiosciences.com/pdfs/whitePapers/07-A790030-19A.pdf.

Auto-Focus Methods

Auto-focus methods that utilize combinations of hardware and software to find the proper Z plane for image capture are used by automated imaging systems that move from well-to-well or within wells. Regardless of the method used, auto-focus settings must be optimized to accommodate assay parameters such as cells of varying Z depth or probes localized to different subcellular regions (nucleus and plasma membrane). BD Pathway systems have two different auto-focus modes: laser-based and image-based. Laser-based auto-focus identifies the imaging well surface/liquid interface and subsequently moves a fixed Z distance up from the interface to the calculated plane of focus for image capture. Image-based auto-focus uses fluorescence intensity and contrast values from a Z stack of the sample to determine the optimal plane of focus. Both auto-focus methods allow optimization through user-defined settings. It may sometimes be useful to combine the two methods, for example, when the optimum focal plane of a sample deviates from a single fixed Z position (such as in montages that span large distances, with cell types that grow in 3-D, or in matrices that have uneven thickness).

Laser-based auto-focus is faster than image-based auto-focus and can significantly decrease image acquisition time. Image-based auto-focus, however, offers the ability to perform dye-based focusing, which allows independent focusing on objects labeled with different fluorophores. Image-based auto-focus requires illumination of the sample, which, if used extensively, can photobleach fluorescent signals. Therefore, image-based auto-focus mode may not be appropriate for imaging of photolabile probes and dyes.

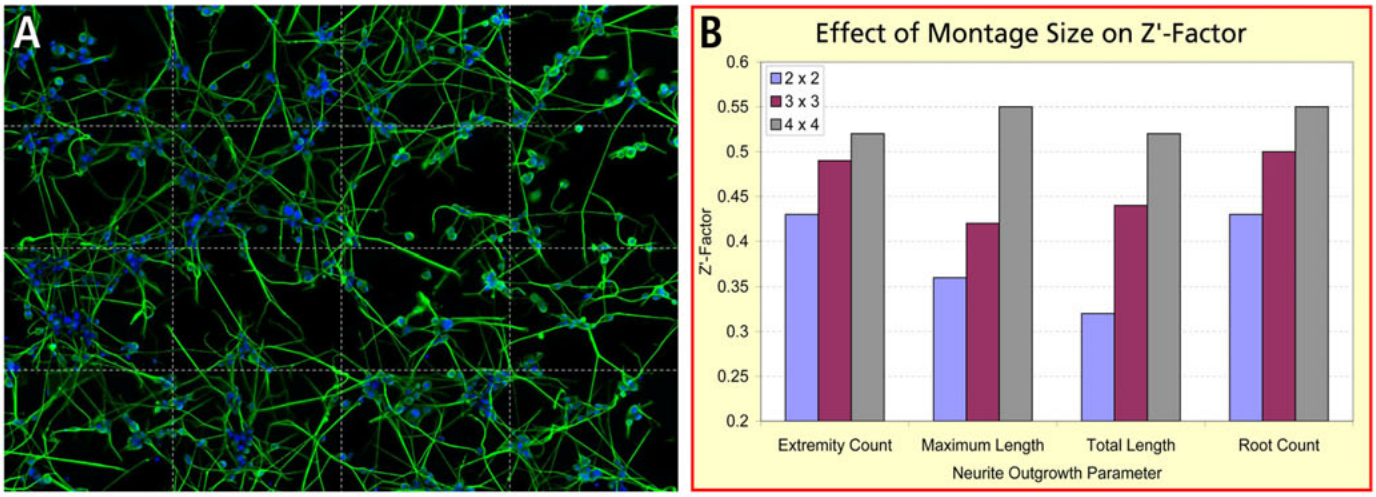

Figure 10. Effect of montage size on assay performance in the Neurite Outgrowth application. A min/max experiment using 48 untreated and 48 NGF-treated (100 ng/mL NGF) wells of PC12 cells was prepared and imaged in nonconfocal mode using different montage sizes. Image data was analyzed using the BD AttoVision™ Neurite Outgrowth software module, and Z′-factor was calculated for various parameters. Montage images of 2 x 2, 3 x 3, and 4 x 4 contain 4, 9, and 16 adjacent image fields, respectively. A 4 x 4 montage consisting of 16 adjacent image fields (denoted by white dashed lines) is shown in Panel A. A plot of the Z′-factor values for four parameters obtained from analyses of images of various montage sizes is shown in Panel B. Images were acquired using a 20x (0.75 NA) objective on a BD Pathway 855.

Confocal Z Stack

Some high-content applications require high-image resolution not only in the X and Y dimensions but also in the Z dimension. In these instances, confocal imaging offers several distinct advantages over conventional wide-field fluorescence imaging. Imaging in confocal mode removes out-of-focus haze by passing light through an optical pinhole, which results in the capture of greater axial resolution (along the Z axis) of the sample. In addition, confocal imaging allows the collection of a Z stack or series of high-resolution optical sections through a specimen. The Z stack can be used to reconstruct the 3-D volume of the sample, or it can be collapsed into a single 2-D image for further analysis. The confocal collapsed Z stack image produces a sharp in-focus representation of the entire thickness of the sample. This is especially useful for assays such as tube formation (angiogenesis) where cell structures form throughout a thick ECM. For further detail, refer to application note "An Image-Based Assay of Endothelial Cell Tube Formation as a Model of Angiogenesis" available at: bdbiosciences.com/pdfs/whitePapers/06-A790030-3A1.pdf. The benefits of using confocal collapsed stack for dense primary neural networks is also discussed in the previously referenced neurite outgrowth application note.

The Z resolution (a measure of resolving power in the Z dimension) of an imaging system must be taken into account when defining Z step sizes. Z resolution is measured using the point spread function (PSF), which describes the response of an imaging system to a point source or point object.[5] The measured Z resolutions using the PSF for three objectives on a representative BD Pathway™ 855 system were:

60x (1.4 NA) = 0.8 microns

40x (0.9 NA) = 2.0 microns

20x (0.75 NA) = 2.8 microns

To properly represent the axial detail of a sample, the Z step spacing should be approximately half the Z resolution of the system. For instance, when using a 40x (0.9 NA) objective on the BD Pathway 855 where the Z resolution was measured as 2.0 microns, imaging should be performed with 1.0 µm Z steps.

An example of how confocal imaging can improve the performance of a high-resolution imaging assay is illustrated by the DNA damage data shown in ***Figure 11***. In this assay, when imaged in confocal collapsed Z stack mode, nuclear foci had sharper boundaries that allowed better identification of individual foci as compared to wide-field (nonconfocal) imaging mode. This translated into higher accuracy and assay robustness. For further detail, refer to the "DNA Damage and Repair - Quantification of Sub-Cellular Events Using Automated Confocal Imaging" application note available at: bdbiosciences.com/pdfs/whitePapers/06-A790030-6A1.pdf.

Table 6 provides a summary of the advantages and disadvantages of the various image acquisition factors that have been discussed. Although there are many important factors to consider and optimize during the biology and image acquisition stages, it may not be necessary or possible to find one combination of conditions that produces the perfect set of images. The important point is to determine the assay requirements (or tolerances) that produce biologically and statistically relevant results for each application.

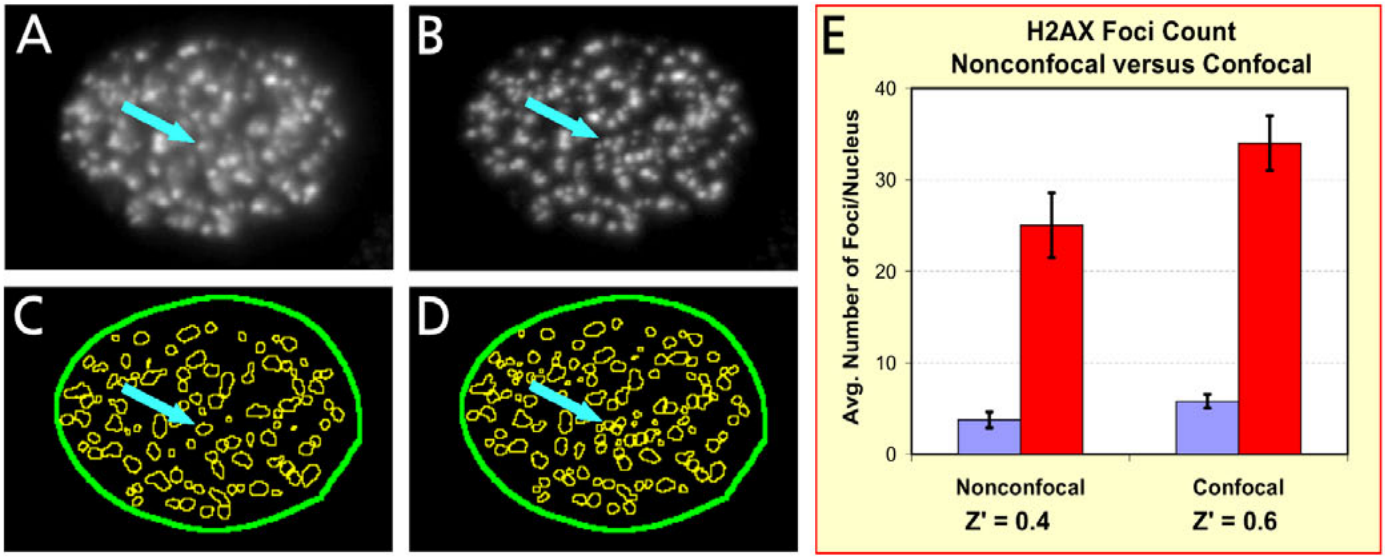

Figure 11. Comparison of nonconfocal and confocal acquisition modes. HT-1080 cells were treated with hydrogen peroxide and processed for staining with an antibody detecting a phosphorylated form of H2AX (a specialized form of the histone H2A protein that accumulates at DNA double-strand breaks). In nonconfocal mode (Panel A), nuclear foci appeared fewer in number, larger, and blurred compared to a collapsed confocal Z stack (Panel B). Confocal imaging resulted in the identification of a greater number of individual foci (arrow) and improved image segmentation (Panels C and D). Panel E shows the average number of nuclear foci, control values (blue bars) were compared to treated wells (red bars). Assay performance was measured as Z'-factor values for the average number of nuclear foci, which were 0.4 for nonconfocal and 0.6 for confocal, collapsed stack images. N = 6 wells ± SD. Images (cropped) were acquired using a 40x (0.9 NA) objective on a BD Pathway™ 855.

Table 6. Advantages and disadvantages of BD Pathway™ image acquisition modes and options.

Option	Advantages	Disadvantages
40x magnification	High-NA and LWD options available High-spatial resolution	Reduces image field size
20x magnification	High-NA and LWD options available Works well for most imaging needs	Small subcellular features may not be fully resolved
10x magnification	Captures 4–fold more cells per image than 20x	Low resolution
4x, 2x magnification	Large image field enables imaging of larger numbers of cell and model organisms	Low resolution
Long-pass filter sets	High-light throughput	Potential for bleed-through (when multiplexing)
Band-pass filter sets	Narrower range allows multiplexing	Potential for pixel shift
Multiband-pass filter sets	Allows multiplexing	Low-light throughput Potential for bleed-through
Camera gain	Increases signal intensity	Increases background noise
Pixel binning	Increases signal intensity	Lowers image resolution
Montage mode	Captures contiguous (or noncontiguous) image fields Increases sample size	Increases image acquisition and image analysis time
Laser-based auto-focus	Increases plate throughput No photobleaching of sample	Fixed offset position requires optimization for each plate/objective combination
Image-based auto-focus	Dye-based Tracks samples at variable distances from the plate bottom	Decreases plate throughput Photobleaches sample
Wide field	Works well for many applications Allows imaging of dim samples	Images contain light from above and below the focal plane
Confocal	High-image resolution 3-D reconstruction Sharper images	Increases exposure time Requires bright samples
Confocal collapsed Z stack	3-D information in a 2-D image Increases depth of analysis	Increases imaging time

Stage 3 – Image Analysis

Once images are acquired, the next stage of high-content imaging is image analysis. Image analysis consists of a series of image processing and segmentation steps designed to extract quantitative data from images. Image processing is the application of algorithms, such as flat field correction, background subtraction, and shade correction to improve images for segmentation of cellular features of interest. Segmentation primarily consists of the application of intensity thresholds to define cellular regions (also called regions of interest or ROIs) where measurements will be made. Proper segmentation can be the key to generating meaningful data and must be optimized for every high-content application.

There are a large number of image analysis tools available which can be combined and used to optimize an image analysis method. Each step of the analysis method can be tested on a small set of representative images from the experiment. However, the optimized method must work across all the images in the experiment. This can be especially challenging when a cell treatment dramatically changes the appearance of the cells or objects being measured (for example, in an apoptosis assay). In some cases, an image analysis method can compensate for flaws in both biology and image acquisition. In other cases, however, the use of image processing to correct minor defects is unnecessary, since the imperfections have little or no effect on assay results. This section briefly discusses a few of the more commonly used image analysis methods and provides a framework for further experimentation. The *Image Processing Handbook* by John C. Russ is an excellent resource for a more in depth discussion of image processing techniques.[6]

Image Processing

An initial step of image processing often involves the removal of artifacts in the image. The primary sources of image artifacts are the biology (including autofluorescence from a variety of sources, cell debris, and fluorescent foreign objects) and noise inherent to the imaging system (such as lamps, filters, objectives, mirrors, or camera). The presence of nonspecific background noise in images makes segmentation and identification of specific fluorescent signals of interest more difficult and inconsistent. Removal of these artifacts allows for better segmentation and more accurate measurements of biological responses. Some image processing steps (such as shade correction) alter images to improve segmentation. These images usually are not used for image analysis since the processing modifies pixel intensities in ways that would not be valid for most intensity-based measurements. Images generated from these types of processing steps, however, can be used to generate ROIs or to make morphometric measurements of cellular structures. Extensive image processing can significantly increase the time it takes to perform image analysis. In addition, to allow maximum flexibility for future image re-analysis, original image data always should be maintained in its unprocessed state (this is automatically done on BD Pathway™ systems). As needed, processed images can be generated and saved by the system software. Although a multitude of image processing techniques are available, a typical sequence of steps may include a combination of any of the following:

- Flat field correction
- Background subtraction
- Other preprocessing filters

Flat Field Correction

Flat field correction is an image processing method designed to correct uneven illumination across the image field or shadows generated from the imaging system. These artifacts may arise from misaligned optics, fingerprints, or dust, and can be caused by any element in the optical light path. Flat field correction generally involves the capture of a reference image of the light path. The reference image is then used to correct each image captured with the same or similar light path. Flat field correction can improve image quality and data resolution by making intensity measurements across each image field more accurate. The impact of flat field correction on images is shown in ***Figure 12.***

Background Subtraction

In addition to system-derived noise, images can contain signals from elements other than the objects of interest, such as, autofluorescence from culture medium, buffers, compounds, reagents, or from imaging plates. In live-cell experiments, fluorescent dyes often leak out or are transported out of the cells over time and contribute to nonspecific background fluorescence of the sample. Background subtraction is the process of subtracting this nonspecific background fluorescence to eliminate its effect on image segmentation and measurement. Background subtraction can be applied to an experiment in a variety of ways. For example, a constant pixel value can be subtracted globally from every pixel in each image. This constant pixel value can either be a user-defined value or determined automatically based on image pixel intensities. Alternatively, a reference image can be captured of the background and subtracted from every image. Other types of background subtraction methods (such as rolling ball background subtraction) modify each image of an experiment differently. The rolling ball background subtraction method processes each image based on operations that are defined by the pixel values of a small surrounding region of the image. This type of local background subtraction may alter pixels in one part of an image differently than in another part. An example of how the rolling ball background subtraction method can be used to eliminate an artifact and improve image segmentation is shown in ***Figure 13***.

Other Image Processing Filters

There are a wide variety of other image processing filters that can be applied to images to improve segmentation. Testing different combinations of filters is an important part of optimizing the image analysis process. BD AttoVision™ v.1.6 software provides the following groups of image processing filters:

- Shade correction – evens out the pixel intensities of objects within images making them uniform (even when they actually vary in intensity).
- Local – a selection of rolling ball filters that generates and subtracts a background image based on a moving circular neighborhood kernel (a small matrix of processing operations) in which each pixel is altered based on contributions from a defined number of adjacent pixels.
- Sharpen – focuses blurred images by increasing the contrast of adjacent pixels.
- Smooth – a collection of filters that processes images by replacing each pixel with the average of its neighboring pixels.

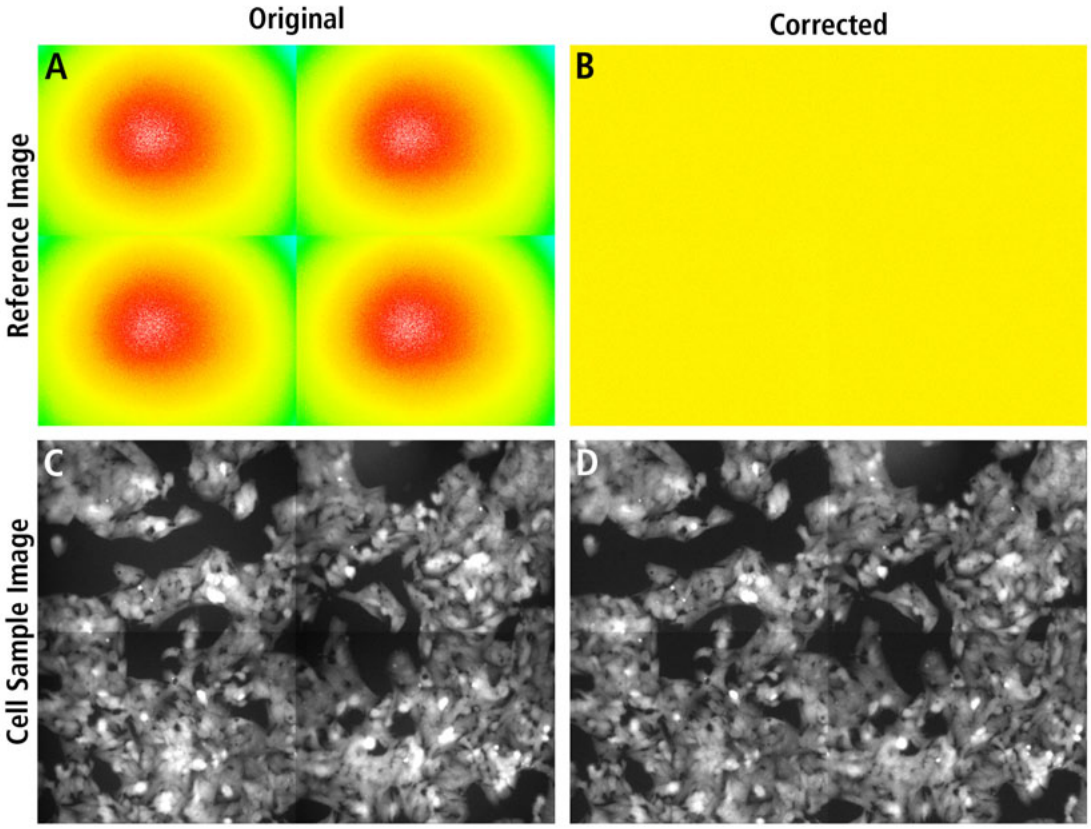

Figure 12. Flat field correction of montage images. A flat field correction reference image was used to correct 2 x 2 images of a flat field reference sample (Panels A and B, pseudocolored using the ratiometric intensity scale) and cells (Panels C and D). Original images are shown in Panels A and C. Corrected images are shown in Panels B and D. Following flat field correction, signal intensities were more uniformly distributed. Images were acquired using a 20x (0.75 NA) objective on a BD Pathway™ 435.

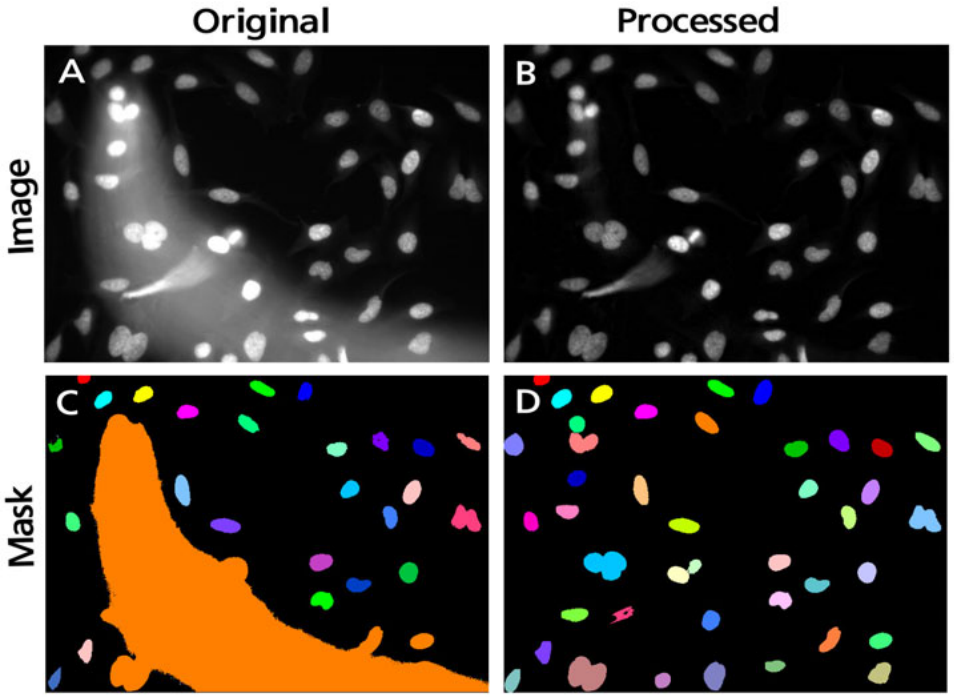

Figure 13. Rolling ball background subtraction improves image segmentation. An image of Hoechst stained HeLa cell nuclei containing an artifact (Panel A) was processed using rolling ball background subtraction (Panel B). The original and processed images were segmented. The segmentation masks are shown in Panels C and D, respectively (colors randomly assigned). In the unprocessed image, the artifact was identified as an ROI, as were the surrounding cells. In the processed image, only the cells in the image field were identified as ROIs. Images were acquired using a 20x (0.75 NA) objective on a BD Pathway 855.

Segmentation

After image processing, the next step in image analysis is segmentation. Segmentation is the process of identifying, separating, and defining objects in images as distinct elements. This is typically accomplished by applying an intensity-based threshold to the image. For fluorescent images of cells, the threshold intensity is the image gray value below which image data is determined to be background and above which the data is considered foreground or part of the objects of interest. Once the threshold is set, objects containing pixel intensities above the threshold are identified and defined by a segmentation boundary or ROI. On BD Pathway™ systems, the threshold intensity value can be determined manually or automatically. A manual threshold is a single user-defined intensity value that is applied to the entire experiment. An automatic threshold is adjusted based on individual image content and typically varies between images of an experiment. Thresholding must be applied appropriately across all images of the experiment. Therefore, automatic thresholding is generally recommended for most high-content imaging applications because compound treatment can have a dose-dependent effect on image background intensity.

In BD AttoVision™ software, the threshold is automatically determined using a multilevel analysis of the image intensity histogram. The histogram analysis can be performed using up to five levels of intensities. Intensity levels are defined by image regions (pixels) of similar intensity. Automatic thresholding using one level (the highest intensity) defines a boundary around the brightest objects in the image (for example, the nucleus). Each increase in number of levels yields a progressively lower threshold intensity value. For example, the use of two or more levels defines boundaries around successively dimmer objects (cytoplasm and plasma membrane). The number of automatic threshold levels should correlate with the number of intensity levels observed in the image and the number of subcellular regions required for proper analysis of the application. An example of automatic multilevel thresholding on a cell image is shown in ***Figure 14***.

Since drug treatment can dramatically alter the morphology of cells, it is likely that in some assays the optimal segmentation method for control and treated cells may differ. Under certain conditions, segmentation using multilevel automatic thresholding can compensate for these morphological changes. This is demonstrated using an apoptosis assay (***Figure 15***). In this example, the nuclei of untreated control cells had a relatively even high-intensity stain with high contrast over a dark background, and nuclei in drug treated cells were fragmented with small regions of high intensity surrounded by dimmer nuclear regions. Using one level automatic thresholding, control nuclei were adequately segmented, but in treated cells, many of the nuclear fragments were identified as individual ROIs which over-represented the cell count. Automatic thresholding using two levels was successful for both the control and treated cells. In the control cells, the high contrast between the nuclei and background still enabled proper segmentation. In the treated cells, an intensity level above background existed between the bright nuclear fragments enabling a single nuclear ROI to be created around each local area of fragmentation. This properly delineated the formerly intact nuclei and provided an accurate cell count.

Segmentation methods are chosen and applied based on the output ROIs they generate. ***Table 7*** lists the segmentation methods available in BD AttoVision v.1.6 software. In most but not all cases, the nucleus is used as a seed for segmentation due to the ability to separate adjacent nuclei better than separating cytoplasm of adjacent cells. *Polygon* is generally used when measurements within a single region (for example, nucleus or whole cell) are desired. *Ring* creates a ring-shaped ROI (of user-specified pixel width) around a central cell area (usually the nucleus). Both *Polygon* and *Ring* perform thresholding on an image of a single fluorescent color channel. The *Ring* shape also can be used with two outputs to simultaneously measure inside the central region (nucleus) of the ring and within the outer ring region (perinuclear or cytoplasm).

Dual Channel segmentation performs thresholding using images of one or two fluorescent color channels. The first channel (Channel A) is usually used to identify nuclei, and the second

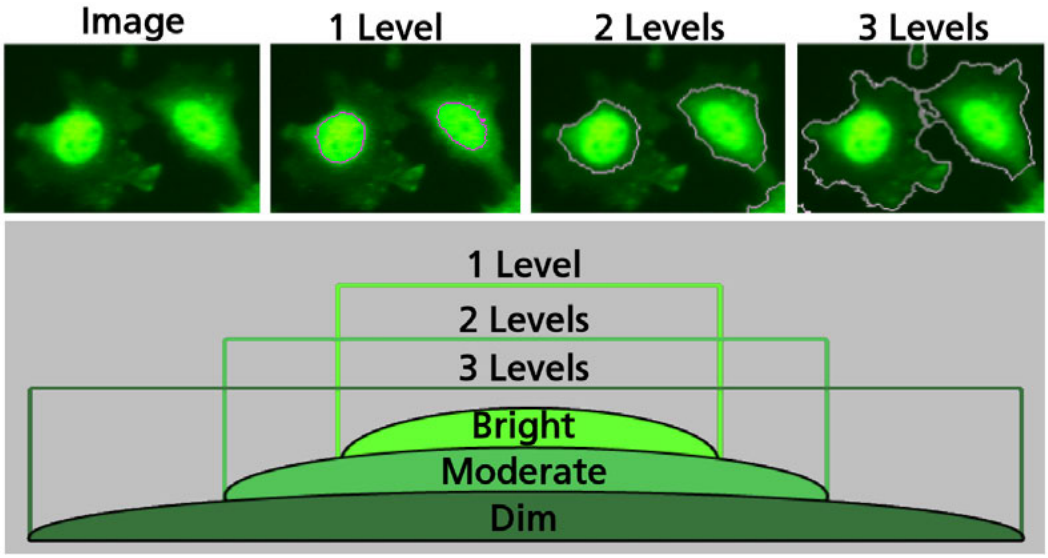

Figure 14. Automatic multilevel thresholding. A cropped pseudocolored image of fluorescently labeled cells is shown unsegmented and with segmentation boundaries applied using 1 Level, 2 Levels, and 3 Levels automatic thresholding (top). An illustration of the intensity levels within a single cell is shown on the bottom.

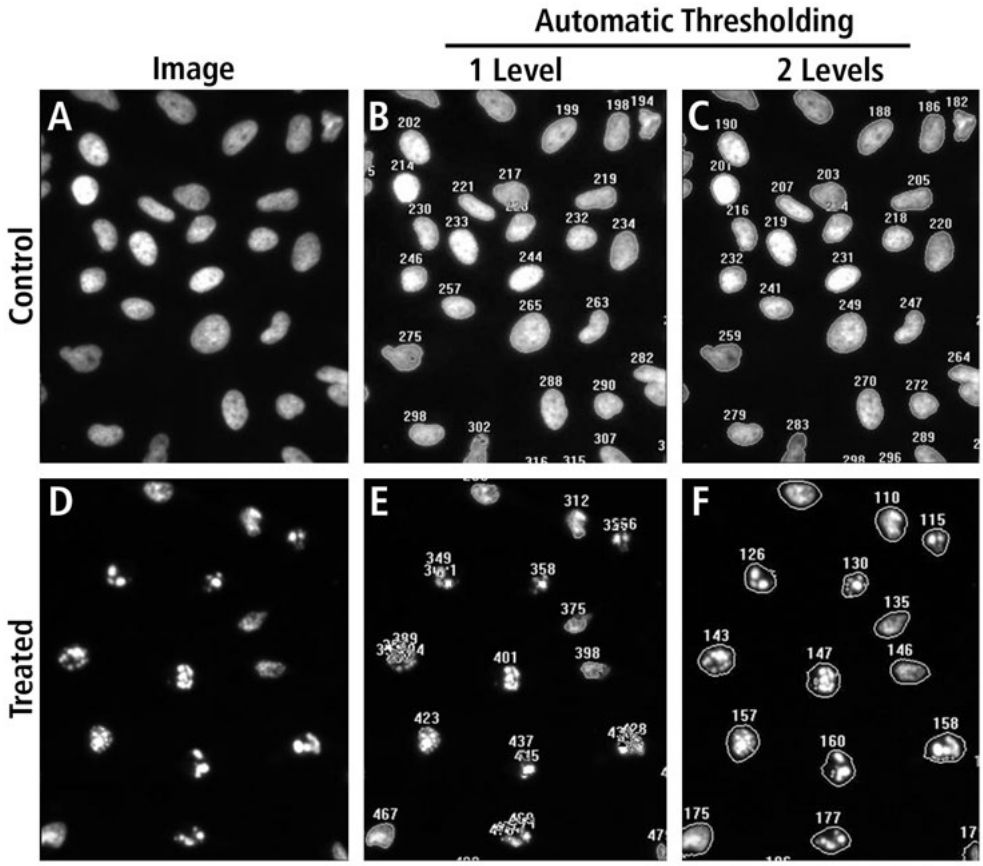

Figure 15. Adjusting the level of automatic thresholding improved the quality of the segmentation. HeLa cells were mock treated (Panels A, B, and C) or treated with 1 µM staurosporine for 4 h (Panels D, E, and F). Images (Panels A and D) were segmented using automatic thresholding with one level (Panel B and E) or two levels (Panels C and F). Note the dramatic change in nuclear intensity and morphology in the staurosporine-treated cells compared to the control cells. ROI numbers show the effect of the segmentation methods on cell count. Images (cropped) were acquired using a 20x (0.75 NA) objective on a BD Pathway™ 855.

channel (Channel B) is used to threshold on a dye or probe specifically labeling a cellular component outside the nucleus (for example, the cytoplasm or cell membrane). In addition, *Dual Channel* can be used to segment a single image where both the nucleus and cytoplasm are labeled with a single dye but at different levels of intensity. *Dual Channel* segmentation can be used to measure intensity in the whole cell (including the nucleus) or in the cytoplasm (excluding the signal in the nucleus). Like the *Ring* shape, *Dual Channel (2 Outputs)* can be used to make simultaneous measurements in two subcellular regions.

Table 7. Description of segmentation methods and list of appropriate assays for their use.

Segmentation Method	Description	Representative Assays
Polygon	Single region, cell, or nucleus	Cell cycle
Ring	Perinuclear region defined through dilation from the nucleus	Nuclear translocation
Dual Channel	Whole cell or cytoplasm	Neurite outgrowth
Bands	Subcellular regions defined through dilation or erosion	Protein redistribution to nucleus, cytoplasm, or membrane

New band segmentation features in BD AttoVision™ v.1.6 software broaden the utility of each of the basic segmentation methods by including the ability to erode, dilate, and divide specific ROIs into an inner and outer region. For each channel (Channels A and B), two regions can be measured simultaneously or independently. The outer region is defined by dilation and the inner region is defined by erosion. Using the NF-κB nuclear translocation application as an example (***Figure 16***), intensity measurements were made in both the nucleus and within a perinuclear cytoplasmic ring based on ROIs defined using *Ring (2 Outputs)* and *Ring (2 Outputs) Band*. The ratio of nuclear-to-cytoplasmic ring intensity was calculated and used to evaluate protein translocation from the cytoplasm to the nucleus in response to TNF-α treatment. Since cytoplasmic intensity can vary as the cytoplasm thins out toward the periphery of the cell, perinuclear rings generally are used to define the cytoplasmic ROIs. However, since bright fluorescent signals can bloom from one region (nucleus) into another (cytoplasm), it can be beneficial to remove pixels immediately adjacent to the nuclear boundary from object measurements. Band segmentation can be used to fine-tune the placement of segmented ROIs. ***Figure 16*** shows a comparison of data generated using *Ring (2 Outputs)* and *Ring (2 Outputs) Band* segmentation methods. While EC_{50} values calculated for the two segmentation methods were equivalent (data not shown), band segmentation consistently improved the assay window of the application.

Segmentation also can be influenced by fluorescent artifacts or cell debris that appear in images as objects. These artifacts are often either larger or smaller than the actual objects of interest. It is often useful to eliminate or "scrap" these contaminating

objects from the segmentation process based on size. A minimum scrap size is used to eliminate small fluorescent debris and any objects resulting from noise in the imaging system, while a maximum scrap size is used to eliminate large objects and clumps of cells. ***Figure 17*** shows an example of how scrapping can improve segmentation by removing both small and large artifacts. Note the difference in the end result obtained using scrapping (***Figure 17***) as compared to rolling ball background subtraction (***Figure 13***) to remove a large artifact. In the scrapping method, cells segmented as part of the artifact and cells obscured by the artifact were removed from the segmentation mask leaving a void. Rolling ball background subtraction removed image artifacts prior to segmentation (provided they are dimmer than the objects of interest) allowing all cells to be properly segmented.

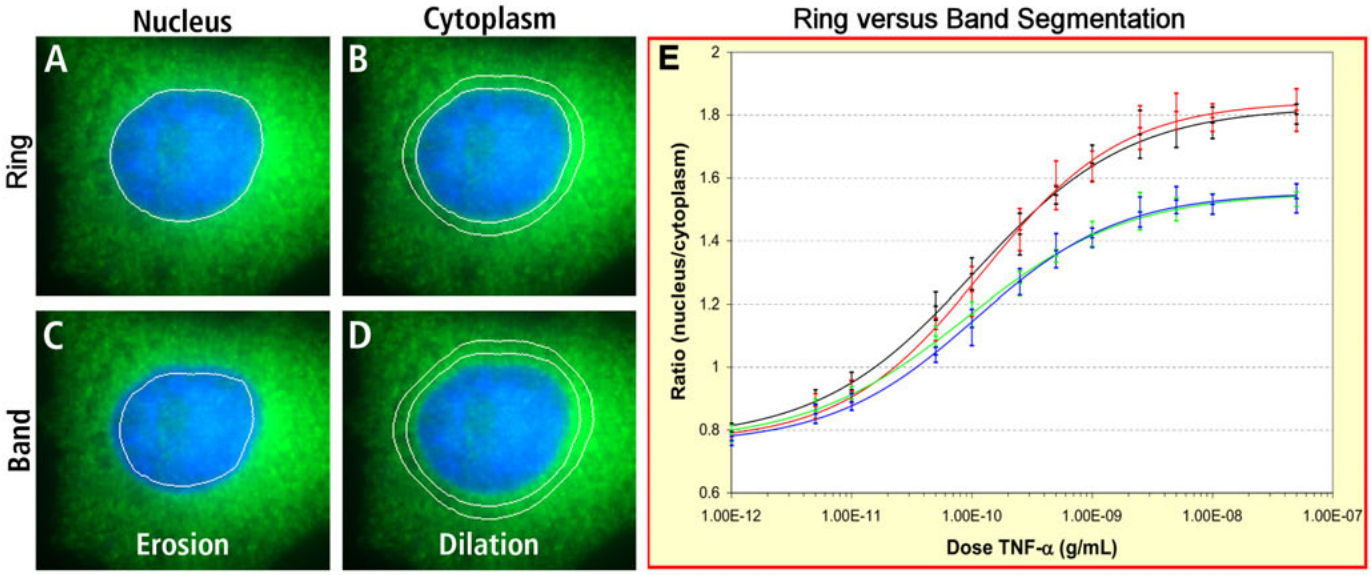

Figure 16. Comparison of ring and band two outputs segmentation methods. Two identical NF-κB assay plates were prepared and imaged. Segmentation outputs were overlaid on a cropped and zoomed image of a single untreated cell acquired using a 40x (0.9 NA) objective. Panels A and B show the ROI outputs for ring segmentation and Panels C and D show the ROI outputs for band segmentation with erosion into the nucleus (Panel C) and dilation into the cytoplasm (Panel D). Panels A and C show the nuclear ROIs and Panels B and D show the cytoplasmic ROIs. Panel E shows dose-response curves comparing ring segmentation (blue and green curves) with band segmentation set to remove two pixels from either side of the nuclear boundary (red and black curves). N = 6 wells ± SD for each plate. Images were acquired using a 20x (0.75 NA) objective on a BD Pathway™ 855.

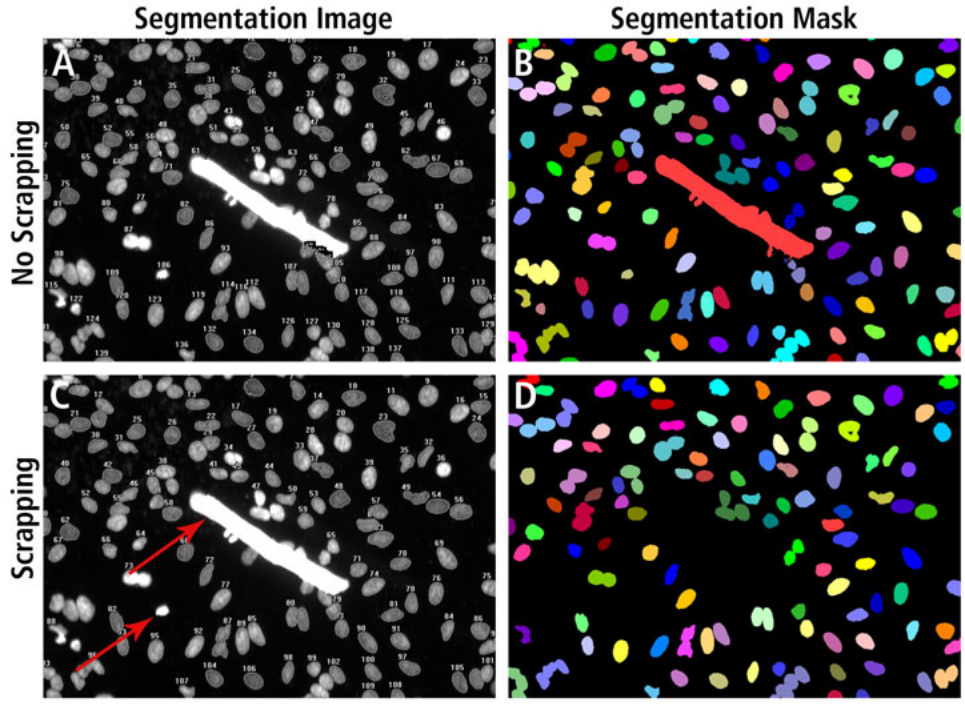

Figure 17. Effect of scrapping on image segmentation. Hoechst stained nuclei were imaged and segmented with and without minimum and maximum size scrapping (300 and 2000 pixels, respectively). Panels A and B show the segmented image with ROI numbers and segmentation mask without scrapping, respectively. Panels C and D show the segmented image with ROI numbers and segmentation mask with scrapping, respectively. Red arrows indicate the ROIs that were removed with size scrapping; these object no longer have ROI numbers associated with them. Images were acquired using a 20x (0.75 NA) objective on a BD Pathway 855.

Measurement Features

Once images are appropriately segmented, a wide variety of features can be measured. Most features can be classified as intensity-based or morphometric-based. Some features, such as average intensity and area, are general and used in most applications. Other features are unique to specific applications. For example, average neurite length, root count, and node points are features specifically measured in the Neurite Outgrowth application. Many new measurement features including morphometric measurements, advanced intensity-based measurements, and measuring objects-within-objects have been added to BD AttoVision™ v.1.6 software. Measurement of multiple features enables a more detailed (high content) investigation of the biological system.

Stage 4 – Data Analysis and Visualization

Interpretation of the results from a high-content imaging application requires proper presentation and visualization of the image data. Many data display options are available using BD Pathway™ software. Image data can be displayed graphically as heat maps, line graphs, bar charts, scatter plots, or dose-response curves. In addition, to interpret data within a plate or set of plates at a glance, thumbnail images of the entire plate can be displayed and feature measurement values viewed as heat maps overlaid onto a multiwell or drug treatment map.

Data Classification

Image data also can be classified into groups based on user-defined threshold values that are specific for any given measurement feature. This makes it possible to quickly identify and localize positive responses from among a series of plates, such as in a drug screening campaign. Data classification also can be run "on-the-fly" to allow immediate visualization of results. ROI and well data can be color coded based on their response levels. ***Figure 18*** shows data classified for a BD™ Bioimaging Certified antibody screening experiment (discussed in the *Biology* section).

Scatter Plots, Parameter Constraints, and Percent Responders

Many biological responses are heterogeneous where only a subpopulation of cells may respond to a cell treatment at any point in time. One way to analyze a heterogeneous biological response is to plot the percentage of cells in the population that demonstrate a particular response. This is achieved by setting a threshold value for a given feature and classifying cells as positive or negative responders based on the threshold. To determine an appropriate threshold, the values of two features can be plotted against each other in a scatter plot. ***Figure 19*** shows an example where the ROIs values from multiple control

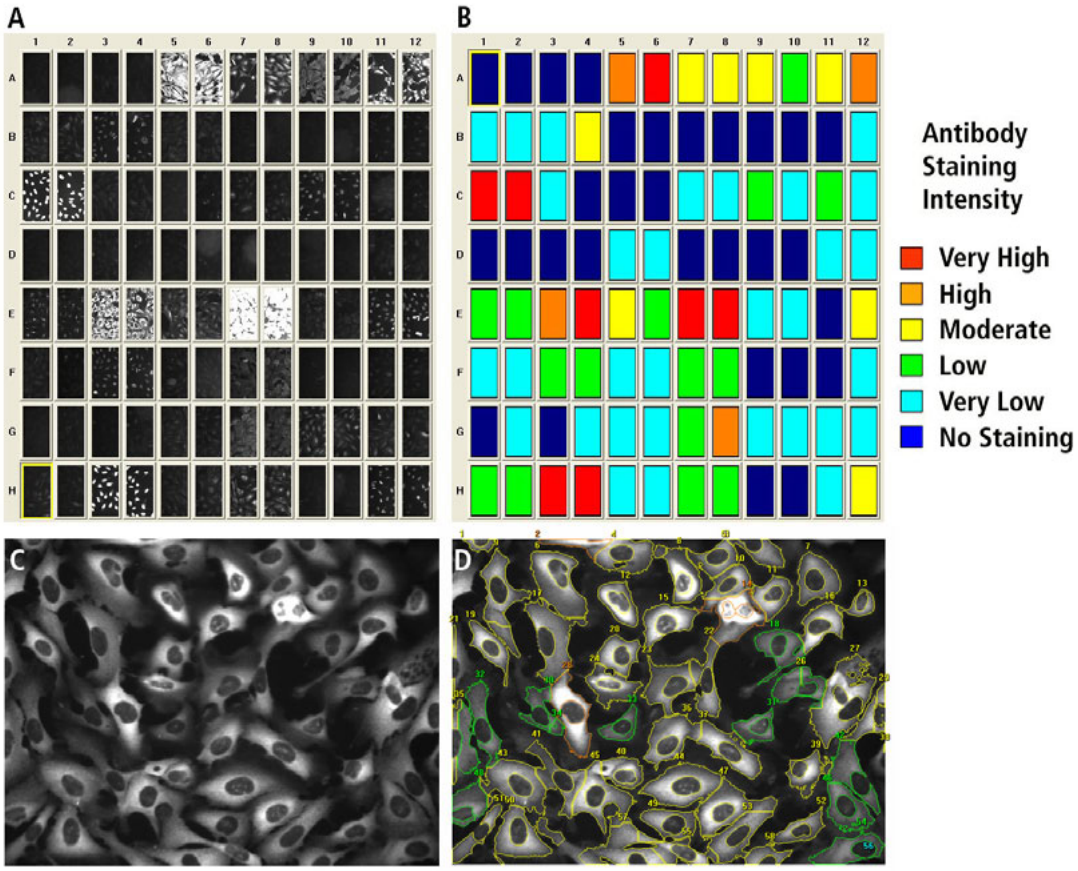

Figure 18. Data classification of antibody screening data. HeLa cells were processed and stained with 47 different antibody specificities and controls in duplicate wells of a 96-well plate. The individual cells and wells were scored and classified into six groups based on antibody staining intensity using BD AttoVision software. Classifications ranged from very high-staining intensity (red) to no staining (dark blue). Thumbnail images of a representative 96-well plate experiment are shown in Panel A with color coded well-based classifications shown in Panel B. A representative image field from a well classified as Moderate (yellow) is shown in Panel C. Panel D shows the classification of the individual cells (note the color coding) based on the average cytoplasmic staining intensity. Images were acquired using a 20x (0.75 NA) objective on a BD Pathway 855.

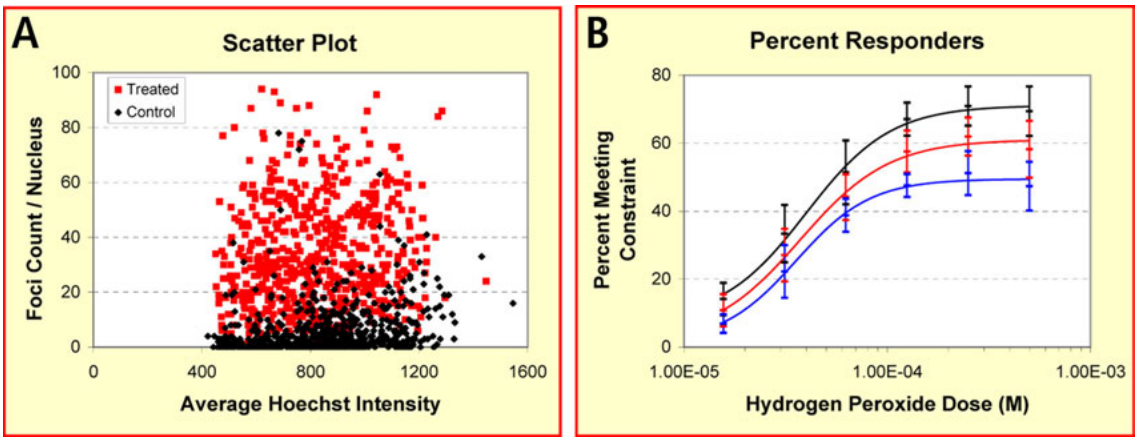

Figure 19. Scatter plots and feature value constraints used to calculate percent responders. HT-1080 cells were exposed to dilutions of hydrogen peroxide (treated) or mock treated for 10 minutes (control). The cells were fixed and processed for staining of nuclei (Hoechst) and nuclear foci (anti-γ-H2AX antibody). Nuclear foci were segmented and counted in individual nuclei using an automated image analysis method (***Figure 11***). Panel A shows a scatter plot of the average nuclear foci count per nucleus versus Hoechst intensity for treated cells (250 µM hydrogen peroxide, black symbols) and control cells (red symbols), N = 6 wells. The majority of control cells fall below 20 average foci. Panel B shows dose-response curves plotting percent responders at each hydrogen peroxide dose where the average nuclear foci count was constrained to various levels including ≥20 (black curve), ≥25 (red curve) and ≥30 (blue curve) foci per nucleus. N = 6 wells ± SD. Images were acquired using a 40x (0.9 NA) objective on a BD Pathway 855.

and treated wells were plotted on the same graph. This allowed the threshold level of response that best separated the two classes to be more easily determined. The threshold value was then used to set a constraint on the experimental data so that the percentage of cells above the threshold (percent responders) could be plotted.

Z′-Factor and Signal-to-Noise Ratio

BD Pathway™ software automatically calculates the Z′-factor and signal-to-noise ratios (SN) for every measurement feature. This permits rank assessment of the effectiveness of the features as measurement tools. Z′-factor is commonly used to assess the screenability or robustness of an assay. When calculated for a submaximal dose, the term is referred to as Z-factor rather than Z′-factor.[4] To calculate Z′-factor, typically, a min/max plate is prepared with half the plate treated with a concentration of a drug sufficient to generate a maximal response for use as positive controls, and the other half mock-treated for use as negative controls. The statistical terms used to calculate Z′-factor and SN include the mean (µ) and standard deviation (σ) of the positive (p) and negative (n) controls (µp, σp, µn, σn, respectively). The equation for Z′-factor is defined as:

$$Z'\text{-factor} = 1 - \frac{3 \times (\sigma_p + \sigma_n)}{|\mu_p - \mu_n|}$$

An assay with a Z′-factor approaching 1.0 occurs when the assay window is very large and standard deviations are very small. Assays with Z′-factors ≥0.5 are considered adequate for screening drug libraries, but this may vary based on the specific assay. If the Z′-factors fall below zero, data points from the positive and negative control wells overlap. Similarly, SN is defined as:

$$SN = \frac{\mu_p - \mu_n}{\sigma_n}$$

Parameters with larger signal-to-noise ratio values show greater separation between control and treated populations. ***Figure 20*** shows an example of a min/max plate prepared using the NF-κB nuclear translocation application.

EC_{50} and IC_{50} Values

The most commonly used measurements to evaluate the potency of drug activity are the half maximal effective concentrations, EC_{50} for agonists and IC_{50} for antagonists. These terms refer to the concentration of a drug that induces a response halfway between the baseline and the maximum response levels. EC_{50} and IC_{50} values should be calculated from carefully prepared dose-response curves. To produce the best results, the curves must contain data points that adequately span the response range. In addition, there must be a sufficient number of replicate wells to minimize inherent biological variability. The dose-response data is fit to a sigmoidal curve using a four parameter logistic model (Hill-Slope model). The curves are then used to determine EC_{50} and IC_{50} values. The equation is defined as:

$$Y = \text{Bottom} + \frac{(\text{Top} - \text{Bottom})}{(1 + (X/EC_{50})(\text{Hill slope}))}$$

where Y is the observed value, Bottom is the lowest observed value, Top is the highest observed value, and the Hill slope gives the largest absolute value of the slope of the curve. For antagonist assays, cells are first treated with a full range of antagonist concentrations and subsequently treated with a submaximal level of agonist capable of inducing a 70% or 80% response level (EC_{70} or EC_{80}).

EC_{50} and IC_{50} curves can be calculated automatically using BD Pathway software. An example of a plate setup for calculation of EC_{50} and IC_{50} values is shown in ***Figure 21***. Two dose-response curves were generated, one for TNF-α and the other for MG-132, an inhibitor of the NF-κB response. For the inhibition assay, cells were pretreated with different concentrations of inhibitor for 30 minutes prior to treatment with an EC_{80} of agonist.

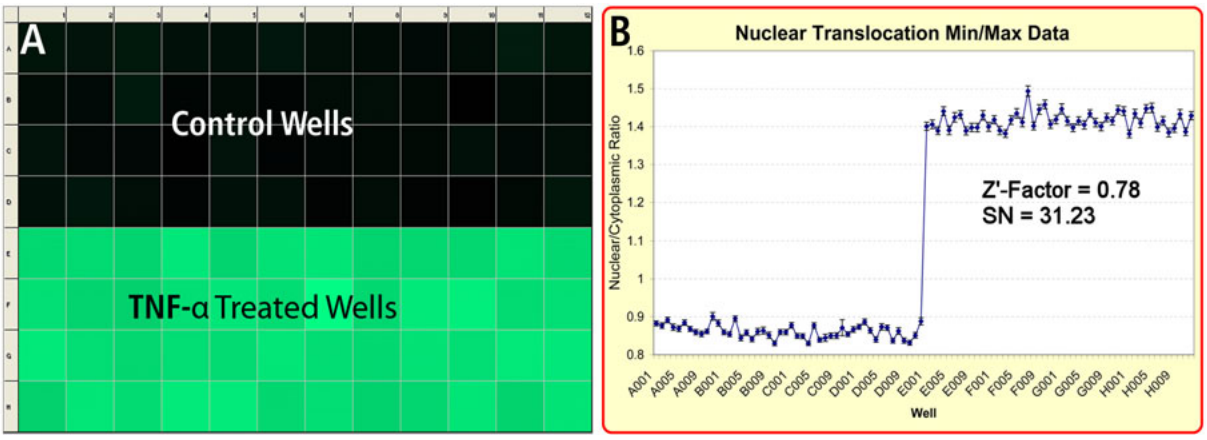

Figure 20. Graphical display of an NF-κB nuclear translocation assay. A min/max plate was prepared with the top half of the plate (N= 48) treated as controls and the lower half of the plate (N = 48) treated with 50 ng/mL TNF-α for 30 min. The cells were processed and stained with an antibody that detects the NF-κB p65 protein. The measurement feature defined as the ratio of the average nuclear intensity to average cytoplasmic intensity for each well was displayed graphically as a heat map (Panel A, dark color = low ratio, light color = high ratio). A line graph (Panel B) was used to plot the ratio values ± SEM for each well. The Z'-factor and signal-to-noise ratio (SN) calculated for this measurement feature by the BD Pathway™ software were determined to be 0.78 and 31.23, respectively.

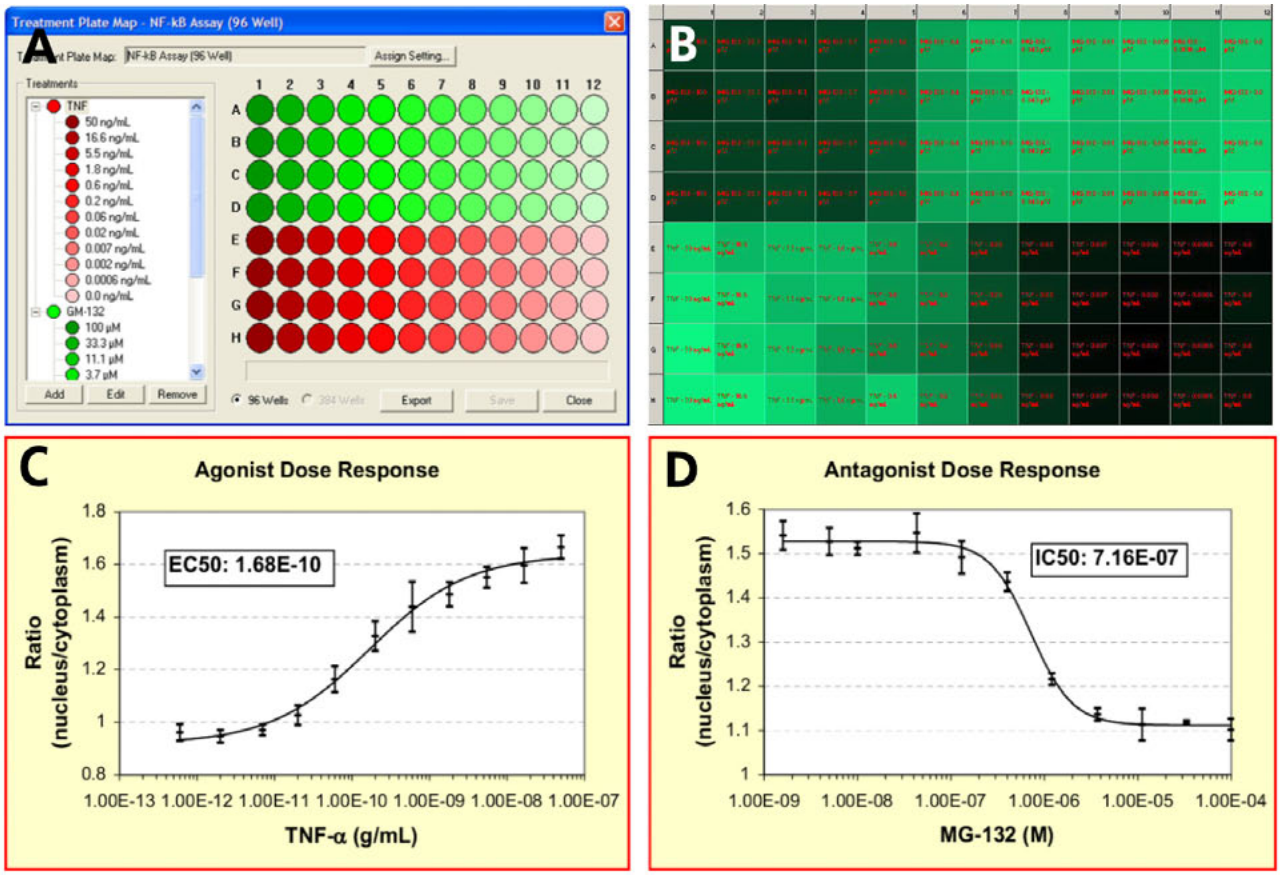

Figure 21. Dose-response curves of NF-κB nuclear translocation. HeLa cells were used in both agonist (TNF-α) and antagonist (MG-132) assays. The antagonist assay was performed at the EC_{80} of TNF-α (3 ng/mL). The cells were processed and stained using anti-NF-κB antibody. A drug treatment plate map (Panel A) was used by the software to label each well with its corresponding drug concentration (red text in Panel B). The ratio of the average nuclear intensity to average cytoplasmic intensity for each well is displayed as a heat map (Panel B, dark color = low ratio, light color = high ratio). BD Pathway software was used to calculate of the EC_{50} of TNF-α (Panel C) and the IC_{50} of MG-132 (Panel D).

Summary

Implementation of a robust high-content imaging application is a complex and time consuming process. There are a large number of factors that can critically affect the results. The process is further complicated because each application is unique and presents a new subset of factors. Those factors having the most significant impact should be optimized. This application note serves as a guide for identifying key factors that potentially have the greatest impact on the successful implementation of high-content imaging.

In an effort to make the entire process more manageable, we divided it into the following four stages: biology, image acquisition, image analysis, and data analysis. Within each stage, we identified a number of key factors that can critically impact assay results. Using specific examples from high-content imaging applications as well as other resource materials, we illustrated and discussed multiple parameters that impact these factors and provided guidance for their optimization. Having a complete understanding of the high-content imaging process will provide a foundation for the development and optimization of new and existing applications.

Our goal is to make navigation of the high-content imaging process easier with specific products and publications designed for this exciting and challenging technology (see *BD Products for High-Content Imaging*).

References

1. Starkuviene V. and Pepperkok R. The potential of high-content high-throughput microscopy in drug discovery. British Journal of Pharmacology. 2007;152:62–71.

2. Passage Number Effects In Cell Lines - Why they happen and what you can do about it. American Type Culture Collection (ATCC) Technical Bulletin. 2007;7.

3. Lundholt BK. A simple technique for reducing edge effects in cell-based assays. Journal of Biomolecular Screening. 2003;8(5):555-570.

4. Zhang JH, Chung TD, Oldenburg KR. A simple statistical parameter for use in evaluation and validation of high throughput screening assays. Journal of Biomolecular Screening. 1999;4(2):67-73.

5. Shaw PJ, Rawlings DJ. The point-spread function of a confocal microscope: its measurement and use in deconvolution of 3-D data. Journal of Microscopy. 1991:163:151-165.

6. Russ JC. The image processing handbook, 4th ed. Boca Raton, Fl: CRC Press; 2002.

BD Products for High-Content Imaging

BD Biosciences provides a complete solution for high-content cellular imaging. The following is a growing list of products and services developed to assist in the implementation of this exciting technology.

Biology

- BD Falcon™ Imaging Plates
  - Tested for flatness
  - Low-evaporation lid
  - Condensation rings
- Extracellular Matrices (BD Biocoat™)
  - Collagen
  - Poly D-Lysine
  - BD Matrigel™
  - Others
- BD™ Bioimaging Certified Reagents and Kits
  - Unlabeled antibodies
  - Fluorescently labeled directly conjugated antibodies
  - Cell Cycle Kit
  - *In-vitro* Micronucleus Assay Kit
  - Fluorescent protein organelle biomarkers
- BD AccuCell™ Automated Cell Counter
  - Image-based technology
  - Viable/nonviable cell counts
  - Disposable cell counting chamber

Image Acquisition

- BD Pathway™ 435 and 855 high-content cell analyzers
  - High-performance laser-based auto-focus
  - Real-time spinning disk confocal
  - High-precision X, Y, and Z movable objectives
  - Full-spectrum light source
  - Temperature and CO_2 controls (BD Pathway 855 only)
  - Liquid handling capabilities (BD Pathway 855 only)

Image Analysis

- BD AttoVision™ 1.6
  - Image Processing
    - Flat field correction
    - Background subtraction
    - Shade correction
    - Other filters
  - Segmentation
    - Manual and automatic thresholding
    - Polygon
    - Ring
    - Dual channel
    - Bands

Data Analysis and Visualization

- BD Pathway Software
  - Data classification
  - Bar charts
  - Scatter plots
  - Dose-response curves
  - Heat maps
  - Cell-by-cell and well-by-well analysis
  - Subpopulations analysis
  - 3-D volume rendering

Technical and Training Support

- Application notes
- Customer support
- Technical application scientists
- Education center
- Custom BD Pathway software services
- Warranty and extended service contract options

BD Bioimaging High-Content Imaging Product Resource List	
Product	Resource Information
BD Falcon Imaging Plates	96-well Cat. No. 353219, 384-well Cat. No. 353221
Extracellular Matrices	bdbiosciences.com/features/products/display_product.php?keyID=265
BD Bioimaging Certified Reagents	1. Go to the following web site: bdbiosciences.com. 2. Search for “bioimaging”
In-vitro Micronucleus Assay Kit	Cat. No. 459001
BD AccuCell Automated Cell Counter	Cat. No. 350300
BD Pathway 855	Part No. 341036
BD Pathway 435	Part No. 641250
Technical Support	1-800-245-2614 (in the USA only)
Training Support	301-340-7320

Notes

Regional Offices

Asia Pacific

Singapore
Tel 65.6861.0633

Australia/New Zealand
Australia
Tel 61.2.8875.7000
Toll Free: 1800 656 100
Fax 61.2.8875.7200
bd_anz@bd.com

New Zealand
Toll Free: 0800 572.468
Tel 64.9.574.2468
Fax 64.9.574.2469
bd_anz@bd.com

Europe
Belgium
Tel 32.53.720.550
Fax 32.53.720.549
customer_service_bdbelgium@europe.bd.com

Canada
BD Biosciences
Toll free 888.259.0187
Tel 905.542.8028
Fax 888.229.9918
canada@bd.com

Japan
Nippon Becton Dickinson
Toll free 0120.8555.90
Tel 81.24.593.5405
Fax 81.24.593.5761

United States
BD Biosciences
Customer/Technical Service
Toll free 877.232.8995
Bioimaging Systems
Fax 301.340.9775
Discovery Labware
Fax 978.901.7493
Immunocytometry Systems
Fax 800.325.9637
Pharmingen
Fax 800.325.9637
www.bdbiosciences.com

Local Offices and Distributors

Argentina/Paraguay/Uruguay
Tel 54.11.4551.7100
Fax 54.11.4551.7400
crc_argentina@bd.com

Austria
Tel 43.1.706.36.60.20
Fax 43.1.706.36.60.11
customerservice.bdb.at@europe.bd.com

Brazil
Unidade Biosciences
Tel 55.11.5185.9995
Fax 55.11.5185.9895
biosciences@bd.com.br

Central America/Caribbean
Tel 502.2 440 4195
Fax 502.2 440 3570

Chile
Tel 56.2 460.0380 x16
Fax 56.2 460.0306

China
Tel 8610.6418.1608
Fax 8610.6418.1610

Colombia
Tel 57.1.572.4060 x244
Fax 57.1.572.3650

Denmark
Tel 45.43.43.45.66
Fax 45.43.43.41.66
bdbnordic@europe.bd.com

East Africa
Tel 254.2.341157
Fax 254.2.341161
bd@africaonline.co.ke

Eastern Europe
Tel 49.6221.305.161
Fax 49.6221.305.418
bdb.ema@europe.bd.com

Egypt
Tel 202.268.0181
Fax 202.266.7562

Finland
Tel 358.9.88.70.7832
Fax 358.9.88.70.7817
bdbnordic@europe.bd.com

France
Tel 33.4.76.68.36.36
Fax 33.4.76.68.35.06
customerservice.bdb.france@europe.bd.com

Germany
Tel 49.6221.305.551
Fax 49.6221.303.609
customerservice.bdb.de@europe.bd.com

Greece
Tel 30.1.940.77.41
Fax 30.1.940.77.40

Hong Kong
Tel 852.2575.8668
Fax 852.2803.5320

Hungary
Tel 36.1.345.7090
Fax 36.1.345.7093
bdb.ema@europe.bd.com

India
Tel 91.124.238.3566.70
Fax 91.124.238.3225

Indonesia
Tel 62.21.577.1920
Fax 62.21.577.1925

Italy
Tel 39.02.48.240.1
Fax 39.02.48.20.33.36

Japan
Fujisawa Pharmaceutical Co., Ltd.
(Reagents from Immunocytometry Systems & Pharmingen)
Tel 81.6.6206.7890
Fax 81.6.6206.7934

Korea
Tel 822.3404.3700
Fax 822.557.4048

Malaysia
Tel 603.7725.5517
Fax 603.7725.4772

Mexico
Tel 52.55.5999.8296
Fax 52.55.5999.8288

Middle East
Tel 971.4.337.95.25
Fax 971.4.337.95.51
bdb.ema@europe.bd.com

The Netherlands
Tel 31.20.582.94.20
Fax 31.20.582.94.21
customer_service_bdholland@europe.bd.com

North Africa
Tel 33.4.76.68.35.03
Fax 33.4.76.68.35.44
bdbiosciences_maghreb@europe.bd.com

Norway
Laborel S/A
Tel 47.23.05.19.30
Fax 47.23.05.19.31

Pakistan
Tel 92.42.5718051
Fax 92.42.5718056
bdb_pak@bd.com

Peru/Bolivia/Ecuador
Tel 51.1.430.0323
Fax 51.1.430.1077

Philippines
Tel 632.815.8981
Fax 632.815.6644

Poland
Tel 48.22.651.75.88
Fax 48.22.651.75.89
bdb.ema@europe.bd.com

Portugal
Enzifarma
Tel 351.21.421.93.30
Fax 351.21.421.93.39

South Africa
Tel 27.11.807.15 31
Fax 27.11.807.19 53
bdb.ema@europe.bd.com

Spain
Tel 34.902.27.17.27
Fax 34.91.848.81.04

Sweden
Tel 46.8.775.51.10
Fax 46.8.775.51.11
bdbnordic@europe.bd.com

Switzerland
Tel 41.61.485.22.22
Fax 41.61.485.22.00
customerservice.bdb.ch@europe.bd.com

Taiwan
Tel 8862.2722.5660
Fax 8862.2725.1768

Thailand
Tel 662.643.1374
Fax 662.643.1381

Turkey
Tel 90.212.328.2720
Fax 90.212.328.2730
bdb.ema@europe.bd.com

United Kingdom & Ireland
Tel 44.1865.78.16.88
Fax 44.1865.78.16.27
BDUK_CustomerService@europe.bd.com

Venezuela
Tel 58.212.241.3412 x248
Fax 58.212.241.7389

West Africa
Sobidis
Tel 225.20.33.40.32
Fax 225.20.33.40.28

BD Biosciences
10975 Torreyana Road
San Diego, CA 92121-1106
Toll free 877.232.8995
bdbiosciences.com

07-A790030-21A